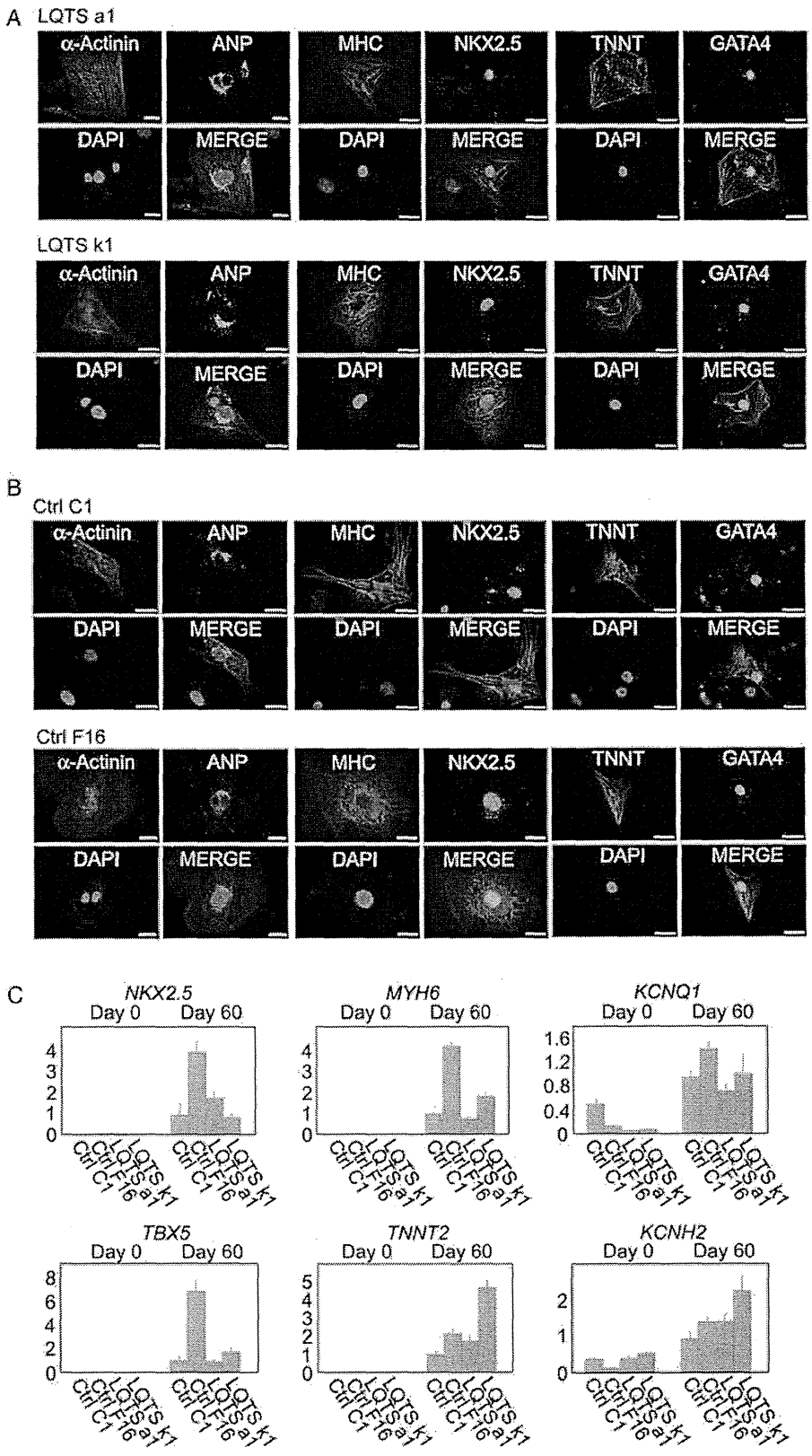

Figure 2 Cardiomyocyte generation from control- and LQTS-iPSCs. (*A*) and (*B*) Immunofluorescence staining for cardiac markers (α-Actinin, ANP, MHC, NKX2.5, GATA4, and TNNT) in the LQTS- and control-iPSC-derived cardiomyocytes. Scale bar, 20 μm. (*C*) Quantitative RT–PCR analyses for cardiac markers (*NKX2.5*, *TBX5*, *MYH6*, and *TNNT2*) and ion channels (*KCNQ1* and *KCNH2*) in the control- (Ctrl) and LQTS-iPSC, and in iPS-derived EBs at day 60.

Downloaded from http://cardiovascres.oxfordjournals.org/ at Shiga University of Medical Science Library on February 5, 2013

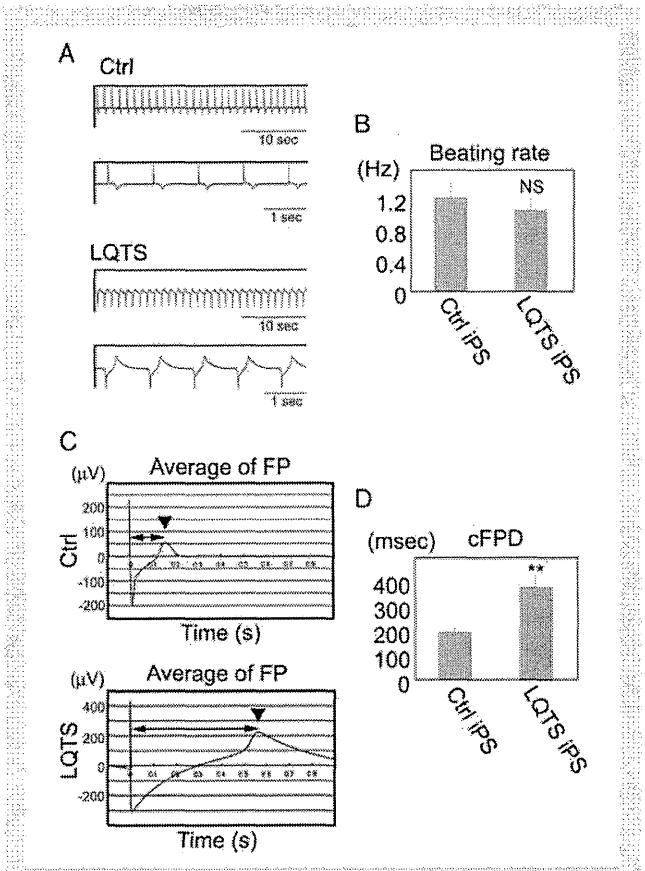

Figure 3 Electrophysiological features of LQTS-iPSC-derived cardiomyocytes. (*A*) Representative MEA recording from the control- and LQTS-iPSC-derived beating EBs. (*B*) Beating rate of the control- and LQTS-iPSC-derived EBs. (*C*) Average of field potential (FP) recorded by MEA in the control- ($n = 12$) and LQTS-iPSC-derived beating EBs ($n = 12$). Triangle indicates the peak of FP and bilateral arrow indicates the FPD. (*D*) cFPD obtained from the control- ($n = 12$) and LQTS-iPSC-derived beating EBs ($n = 12$).

polymorphic ventricular tachycardia (PVT)-like arrhythmia (*Figure 4D* and Supplementary material online, *Figure S4A*).[27] E4031-induced PVT-like arrhythmias were never observed in control-iPSC-derived beating EBs. We then found that another major repolarization potassium current relating to LQTS, IKs, was blocked by chromanol 293B, which significantly prolonged cFPD in control-iPSC-derived beating EBs, but not in LQTS-iPSC-derived beating EBs (*Figure 4E* and *F*). These data indicated that LQTS-iPSC-derived cardiomyocytes have IKs channel dysfunction and/or chromanol 293B insensitivity. We also examined the inwardly rectifying potassium current IK1 by the IK1-blocking barium administration. The application of barium prolonged FPD in both control- and LQTS-iPSC-derived cardiomyocytes (see Supplementary material online, *Figure S4B*). However, barium administration did not induce arrhythmogenic events in control- and LQTS-iPSC-derived beating EBs. These findings suggested that repolarization of LQTS-iPSC-derived cardiomyocytes would be mainly controlled by IKr. Taken together with IKr and IKs blocker administration, we proposed that IKs channels were not only genetically but functionally impaired and that IKr channels compensated for this effect in the patient-derived iPSCs, which is also known as the repolarization reserve in cardiomyocytes.[28,29] IKs channel impairment is diagnosed as type 1 LQTS. And it is well known that β-stimulant increases the risk of fatal arrhythmia and that β-blockers would effectively prevent long-QT-related arrhythmia in type1 LQTS.[30] The β-stimulant isoproterenol increased the beating rate in a dose-dependent manner in control and LQTS cells, and induced EAD and ventricular tachycardia (VT)-like arrhythmogenic events in LQTS-iPSC-derived beating EBs (see Supplementary material online, *Figure S5A* and *B* and *Figure 4G*). Interestingly, the non-selective β-blocker propranolol obviously decreased the incidence of arrhythmogenic events (*Figure 4H*). These data strongly suggested that our patient has a functional impairment in the IKs channel system. We confirmed a heterozygous deletion mutant in KCNQ1, 1893delC (P631fs/33), was identified in the LQTS-iPSCs (see Supplementary material online, *Figure S5C*).

To confirm a possible dominant-negative role of the *KCNQ1* 1893delC mutation in IKs channel function, we conducted precise electrophysiological characterizations in iPSC-derived cardiomyocytes. IKs currents can be recorded by subtraction of baseline and the IKs blocker (chromanol 293B) addition. In control, chromanol 293B (30 μM) addition apparently decreased the recorded current, and IKs current was recorded by subtraction (*Figure 5A*). In LQTS-derived cardiomyocytes, chromanol 293B addition did not show apparent differences and IKs current was subtly recorded by subtraction (*Figure 5A*). The IKs peak and tail current densities of the LQTS-derived cardiomyocytes were evidently smaller than those of control (*Figure 5B*). To clarify the mechanisms underlying such effects, we examined KCNQ1 protein expression in LQTS-iPSC-derived cardiomyocytes. We conducted immunofluorescent staining using an antibody that recognizes a C-terminal epitope on *KCNQ1* downstream of P631fs/33. Immunostaining in control showed cell peripheral expression of KCNQ1, which suggested normal shuttling of the KCNQ1 protein into the cell membrane (*Figure 5C*). In LQTS-iPSC-derived cardiomyocytes, the KCNQ1 protein was accumulated at the perinuclear cytoplasm and nucleus, instead of at the cell periphery (*Figure 5C*). These data indicated that KCNQ1 expression is downregulated at the membrane peripheral site (*Figure 5D*), which suggests that KCNQ1 1893delC has a dominant-negative effect via a trafficking deficiency.

We showed this patient has a mutation in *KCNQ1* and that LQTS-iPSC-derived cardiomyocytes have a functional disturbance in KCNQ1 channels. However, it remains unclear whether this mutation directly contributed and whether other mutations could be involved in the IKs current disturbance. To test for a pure dominant-negative role of the *KCNQ1* 1893delC mutation in IKs channel function, we also conducted electrophysiological and histochemical characterizations in HEK cells expressing exogenous wild-type and/or mutated KCNQ1. Cells with 100% incorporation of the wild-type *KCNQ1* (WT) gene recorded typical IKs currents and 50% WT *KCNQ1* gene introduction slightly reduced the IKs currents (*Figure 6A*). Introduction of 100% mutant *KNCQ1* genes (P631fs/33) (MT) significantly reduced IKs currents (*Figure 6A*). Moreover, 50% WT and 50% MT gene introductions had dominant-negative effects on IKs current (*Figure 6A*). The IKs peak and tail current densities of the 100% MT and 50/50% WT and MT were evidently smaller than those of 100% WT and 50% WT (*Figure 6B* and *C*). Then we also examined KCNQ1 protein expression in *KCNQ1*-transfected HEK cells. Cells

Downloaded from http://cardiovascres.oxfordjournals.org/ at Shiga University of Medical Science Library on February 5, 2013

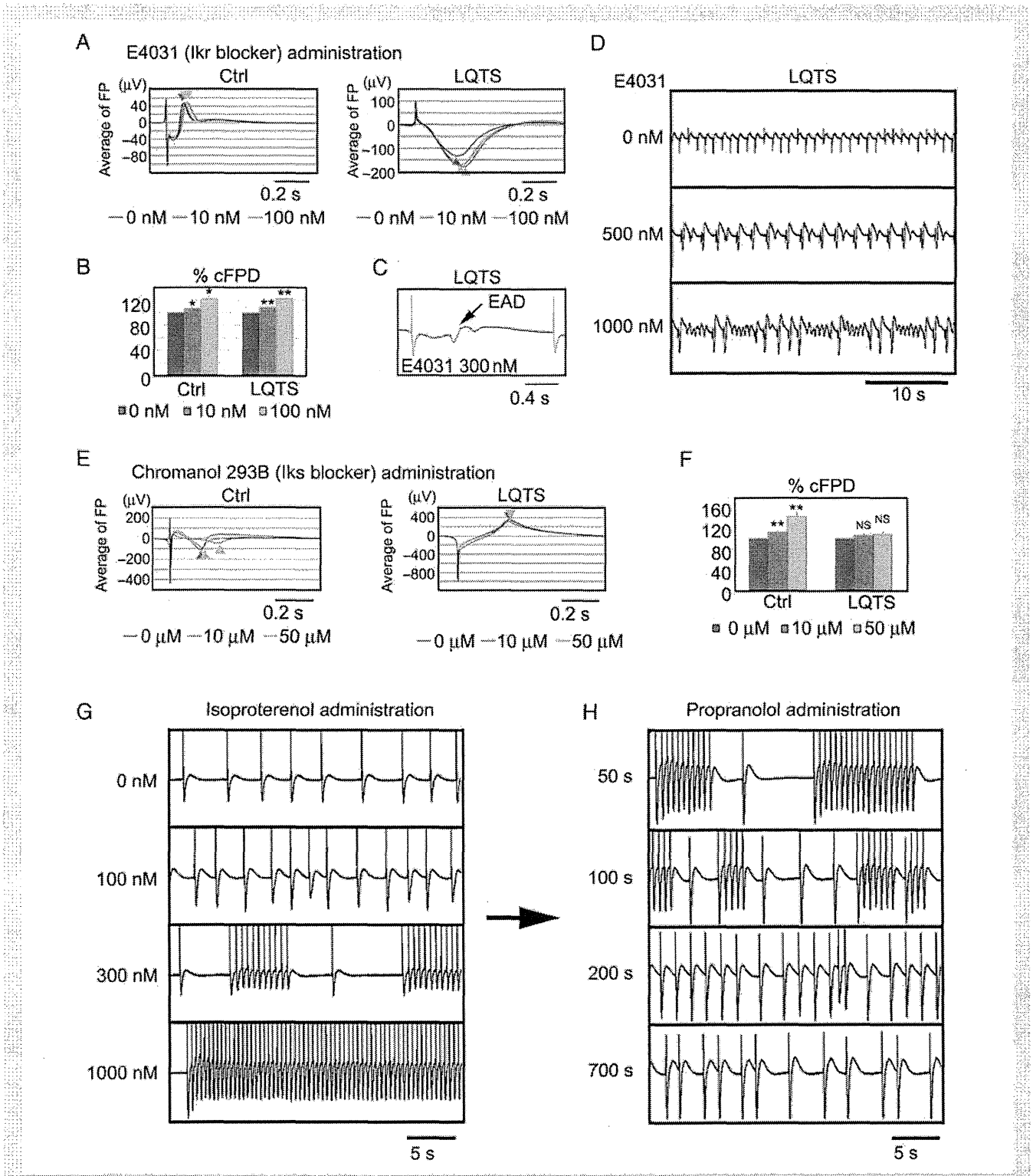

Figure 4 Drug responses of LQTS-iPSC-derived cardiomyocytes. (*A*) Average of FP recorded by MEA after E4031 administration in the control- and LQTS-iPSC-derived beating EBs. Triangle indicates the peak of FP. (*B*) Per cent change of cFPD after E4031 administration obtained from the control- ($n = 6$) and LQTS-iPSC-derived beating EBs ($n = 6$). (*C*) Representative MEA recordings showing EAD after E4031 administration in LQTS-iPSC-derived beating EBs. The frequency of appearing EAD in each cell is control- ($n = 1/16$) and LQTS-iPSC-derived beating EBs ($n = 8/16$). (*D*) Representative MEA records showing PVT-like arrhythmia after E4031 administration in LQTS-iPSC-derived beating EBs. (*E*) Average of FP recorded by MEA after chromanol 293B administration in the control- and LQTS-iPSC-derived beating EBs. Triangle indicates the peak of FP. (*F*) Per cent change of cFPD after chromanol 293B administration obtained from the control- ($n = 8$) and LQTS-iPSC-derived beating EBs ($n = 8$). (*G*) Representative MEA records showing VT-like arrhythmia after isoproterenol administration in LQTS-iPSC-derived beating EBs. (*H*) MEA recordings after propranolol (2 μM) administration in LQTS-iPSC-derived beating EBs during isoproterenol-induced VT-like arrhythmia.

Downloaded from http://cardiovascres.oxfordjournals.org/ at Shiga University of Medical Science Library on February 5, 2013

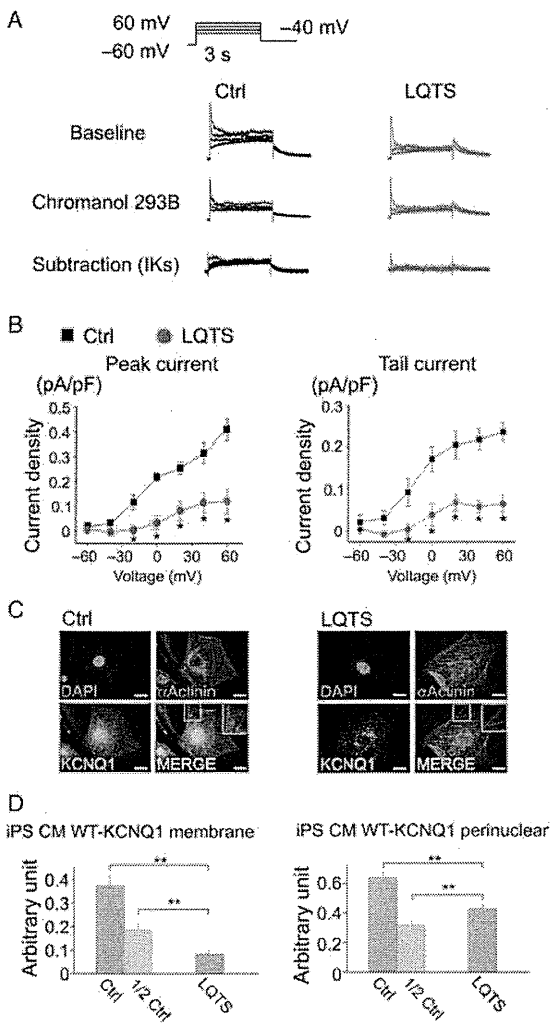

Figure 5 Dominant-negative role of the *KCNQ1* 1893delC mutant in iPSC-derived cardiomyocytes. (*A*) The pulse protocol is shown in the upper panel. Representative current traces of baseline, chromanol 293B (30 μM) administration and subtraction expressed in control- and LQTS-iPSC-derived cardiomyocytes. (*B*) In the left panel, current–voltage relationship of peak current during the test depolarization pulse in control- and LQTS-iPSC-derived cardiomyocytes. In the right panel, current–voltage relationship of tail current upon repolarization to −40 mV following test depolarization in control- ($n = 7$) and LQTS-iPSC-derived cardiomyocytes ($n = 7$). (*C*) Immunofluorescence staining for KCNQ1 and α-Actinin staining in control- and LQTS-iPSC-derived cardiomyocytes. White boxes in each figure are shown at a higher magnification in the inset. Scale bar, 20 μm. (*D*) Densitometric analyses for WT-KCNQ1 expression at membrane peripheral and perinuclear sites in control- ($n = 20$) and LQTS-iPSC-derived cardiomyocytes (CM) ($n = 20$).

carrying 100% WT and 50% WT gene introduction showed cell peripheral expression of KCNQ1, which suggested normal shuttling of the KCNQ1 protein into the cell membrane (*Figure 6D* and *E* and Supplementary material online, *Figure S6*). In contrast, 100% MT and 50/50% WT and MT gene introduction induced KCNQ1 protein accumulation around the perinuclear cytoplasm, instead of at the cell periphery (*Figure 6D* and *E* and Supplementary material online, *Figure S6*). These data indicated that MT-KCNQ1 expression is down-regulated at the membrane peripheral site, which suggests that *KCNQ1* 1893delC has a dominant-negative effect via a trafficking deficiency.

4. Discussion

Human iPSCs have become a promising tool to analyse genetic diseases. Some previous reports indicated that disease-specific iPSCs recapitulated the disease phenotypes.[10–13] However, most patients for generating iPSCs in previous reports were already diagnosed with responsible genes and/or had familial history.[10–13,31,32] We showed here that iPSCs can recapitulate the phenotype of a sporadic patient with LQTS type1. We also performed functional analysis of the novel mutation by using patient-specific iPSCs, which may support the diagnosis of LQTS type 1 with novel mutation. Moreover, using this system allowed us to perform several drug administration tests on the iPSC-derived cardiomyocytes, which would be a realistic risk to such a patient in real medical practice. Patients with LQTS type 1 have to take β-blockers throughout their lives, and thus to confirm that β-blockers truly prevent arrhythmic events in the patients with novel mutations, patient-specific iPSC-derived cardiomyocytes could also be used for drug evaluation and monitoring.

We generated iPSCs from a sporadic LQTS patient with a novel heterozygous mutation located in the *KCNQ1* gene, 1893delC, and differentiated into cardiomyocytes. The electrophysiological function was measured by the MEA system, and we confirmed that cFPD was markedly prolonged in LQTS, as compared with control. Next, we tried to confirm the responsible channel for disease phenotype by precise examination of several drug responses. IKr is responsible for the main potassium current in cardiomyocytes and the IKr blocker significantly prolonged cFPD in LQTS- and control-iPSC-derived beating EBs. But interestingly, we observed more frequently the arrhythmogenic events like EAD in LQTS-derived beating EBs, and PVT-like arrhythmia findings recorded only in LQTS. In addition, IKs is another important potassium current in cardiomyocytes but the IKs blocker did not affect cFPD in LQTS, though it significantly prolonged control's cFPD in a dose-dependent manner. In general, IKr and IKs channels work in a complementary fashion in cardiomyocytes, which is known as repolarization reserve.[28,29,33] Taken together with IKr and IKs administration, we could propose that IKs channels were functionally impaired and that IKr channels would compensate for this effect in the patient-derived iPSCs. It was also supported that the diagnosis of our patient may be LQTS type1 because of the onset of the ventricular fibrillation caused by exertional stress.[20,21] It is important to elucidate whether the disease phenotype is reproducible in the same clinical situation, but it should be better to avoid reproducing ventricular fibrillation in those patients because of the high risk of sudden death. Therefore, we examined whether adrenergic stimulation can cause arrhythmogenic events in LQTS-iPSCs-derived cardiomyocytes. We successfully reproduced that the β-stimulant, isoproterenol, induced VT-like arrhythmia only in LQTS, which was totally blocked by the β-blocker, propranolol. These findings strongly suggested that patient's IKs channels were functionally impaired and we focused on the identification of the responsible gene mutation in the *KCNQ1* gene. To confirm the dominant-negative role of the *KCNQ1* 1893delC mutation in IKs channel function, we examined electrophysiological and histochemical analyses in iPSC-derived

Downloaded from http://cardiovascres.oxfordjournals.org/ at Shiga University of Medical Science Library on February 5, 2013

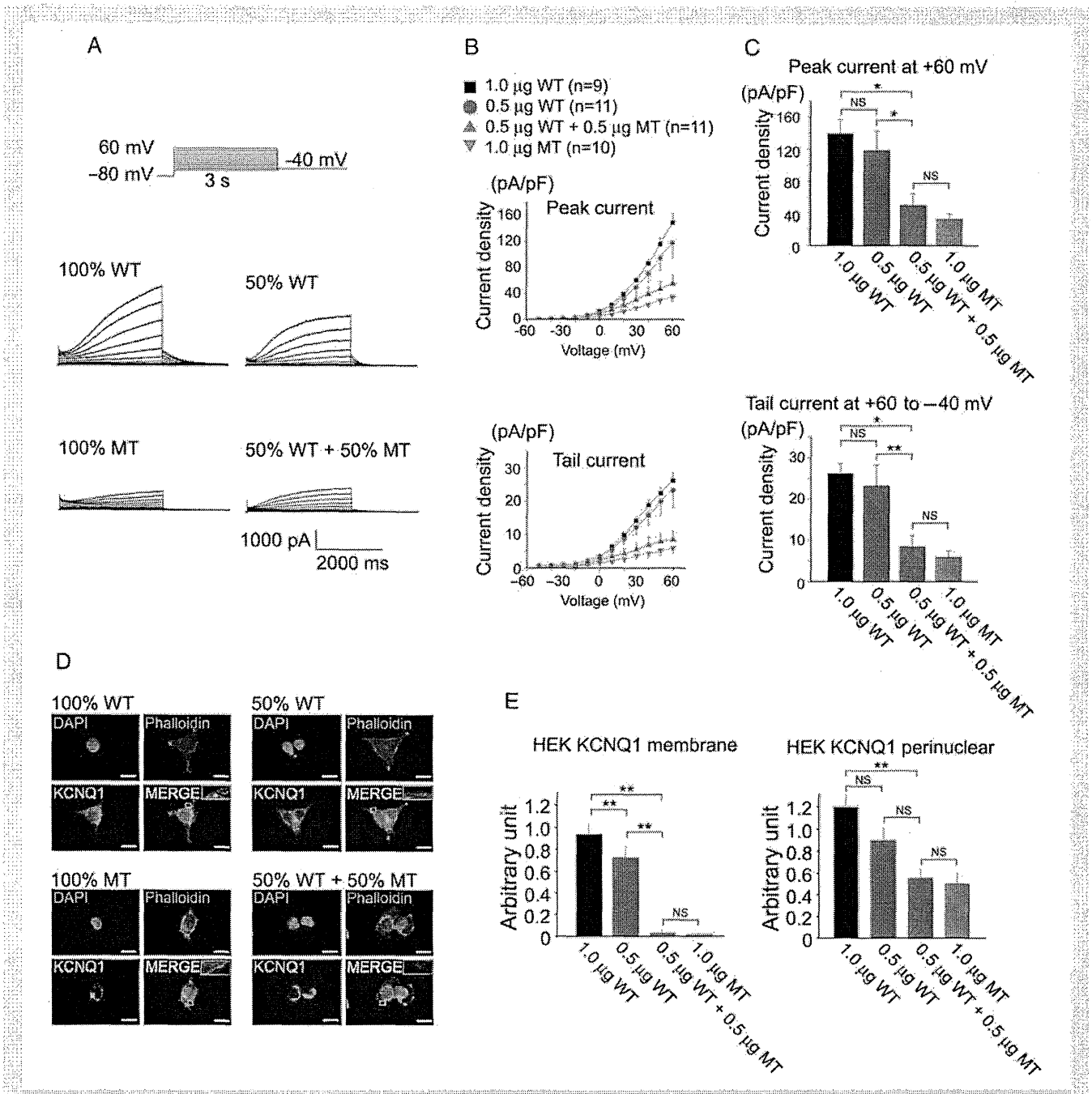

Figure 6 Dominant-negative role of the *KCNQ1* 1893delC mutant in HEK cells. (*A*) The pulse protocol is shown in the upper left panel. Representative current traces of WT- and/or P631fs/33-KCNQ1 expressed in HEK cells. Cells of each panel were transfected as follows: 100% WT-KCNQ1, 50% WT-KCNQ1, 50% WT + 50% P631fs/33-KCNQ1, and 100% P631fs/33-KCNQ1. (*B*) In the upper panel, current–voltage relationship of peak current during the test depolarization pulse in HEK cells introduced with 100% WT, 50% WT, 100% MT, and 50% WT + 50% MT *KCNQ1* genes. In the lower panel, current–voltage relationship of tail current upon repolarization to −40 mV following test depolarization in HEK cells introduced with 100% WT, 50% WT, 100% MT, and 50% WT + 50% MT *KCNQ1* genes. (*C*) Summary of the peak and tail current densities measured following the test depolarization pulse of +60 mV. In the upper panel, bar graphs showing current densities of developing (peak) recorded current at +60 mV. In the lower panel, bar graphs showing current densities of tail current recorded upon repolarization to −40 mV from +60 mV test depolarization. (*D*) Immunofluorescence staining for KCNQ1 and phalloidin staining in HEK cells introduced with 100% WT, 50% WT, 100% MT, and 50% WT + 50% MT *KCNQ1* genes. White boxes in each figure are shown at higher magnifications in the inset. Scale bar, 20 μm. (*E*) Densitometric analyses for KCNQ1 expression at membrane peripheral and perinuclear sites in HEK cells introduced with 100% WT ($n = 14$), 50% WT ($n = 15$), 100% MT ($n = 14$), and 50% WT + 50% MT *KCNQ1* genes ($n = 13$).

Downloaded from http://cardiovascres.oxfordjournals.org/ at Shiga University of Medical Science Library on February 5, 2013

cardiomyocytes, and showed that *KCNQ1* 1893delC has a dominant-negative effect via a trafficking deficiency. And there remains a possibility that other mutated genes might be involved in disease phenotypes. So we examined electrophysiological and histochemical analyses in HEK cells in which WT and MT *KCNQ1* genes were transferred, and showed that *KCNQ1* 1893delC has a dominant-negative effect via a trafficking deficiency.

This study had several limitations with respect to basic research and clinical application. In our study, the control subjects were two healthy volunteers who were unrelated to the patient. The type of such controls that are optimal to use in disease modelling using patient-specific iPSCs remains under discussion.[34] To examine pure functions of the mutated genes, it would seem better to compare patient's family members who do not harbour the mutation, although related family members share genetic information including single nucleotide polymorphisms, and this could affect disease phenotypes. A recent study also showed that ideal control iPSCs can be obtained by mutated gene correction using a targeting strategy.[35] However, it is sometimes difficult to establish iPSCs from family members and correct a mutated gene in human iPSCs. In our study, we used control iPSCs from healthy unrelated volunteers and also performed functional analysis of the mutated genes using gene transduction. Another important issue for routine clinical application of disease modelling using iPSCs is the time path. It takes a few months to generate iPSCs from the patient's dermal fibroblasts, and another few months to differentiate iPSCs into cardiac myocytes. Thus, a minimum of half of year is required to generate iPSC-derived cardiomyocytes that reproduce the patient's phenotype. Although iPSC technology is an attractive tool for analysing human diseases, it is clear that technological innovation remains necessary for the use of iPSCs in routine medical practice.

In the present study, we showed that patient-derived iPSCs could recapitulate disease phenotype in a case of sporadic LQTS. Importantly, this study demonstrated that iPSCs could be useful to characterize the electrophysiological cellular phenotype of a patient with a novel mutation. In terms of effort, cost, and time, such a method for characterizing a phenotype should overcome several problems that remain in realizing the routine clinical application potential of patient-derived iPSC technology, and in turn, the promise of personalized medicine in the future clinical setting.

Supplementary material

Supplementary material is available at *Cardiovascular Research* online.

Acknowledgements

The authors are grateful to Yoko Shiozawa for her technical assistance.

Conflict of interest: none declared.

Funding

This study was supported in part by research grants from the Ministry of Education, Science and Culture, Japan, by the Programme for Promotion of Fundamental Studies in Health Science of the National Institute of Biomedical Innovation and Health Labour Sciences Research Grant.

References

1. Rea TD, Page RL. Community approaches to improve resuscitation after out-of-hospital sudden cardiac arrest. *Circulation* 2010;**121**:1134–1140.
2. Zipes DP, Wellens HJJ. Sudden cardiac death. *Circulation* 1998;**98**:2334–2351.
3. Goldenberg I, Moss AJ. Long QT syndrome. *J Am Coll Cardiol* 2008;**51**:2291–2300.
4. Morita H, Wu J, Zipes DP. The QT syndromes: long and short. *Lancet* 2008;**372**: 750–763.
5. Huikuri HV, Castellanos A, Myerburg RJ. Sudden death due to cardiac arrhythmias. *N Engl J Med* 2001;**345**:1473–1482.
6. Priori SG, Napolitano C, Schwartz PJ. Low penetrance in the long-QT syndrome : clinical impact. *Circulation* 1999;**99**:529–533.
7. Bokil NJ, Baisden JM, Radford DJ, Summers KM. Molecular genetics of long QT syndrome. *Mol Genet Metab* 2010;**101**:1–8.
8. Takahashi K, Tanabe K, Ohnuki M, Narita M, Ichisaka T, Tomoda K *et al.* Induction of pluripotent stem cells from adult human fibroblasts by defined factors. *Cell* 2007;**131**: 861–872.
9. Yu J, Vodyanik MA, Smuga-Otto K, Antosiewicz-Bourget J, Frane JL, Tian S *et al.* Induced pluripotent stem cell lines derived from human somatic cells. *Science* 2007; **318**:1917–1920.
10. Moretti A, Bellin M, Welling A, Jung CB, Lam JT, Bott-Flügel L *et al.* Patient-specific induced pluripotent stem-cell models for long-QT syndrome. *N Engl J Med* 2010; **363**:1397–1409.
11. Itzhaki I, Maizels L, Huber I, Zwi-Dantsis L, Caspi O, Winterstern A *et al.* Modelling the long QT syndrome with induced pluripotent stem cells. *Nature* 2011;**471**: 225–229.
12. Yazawa M, Hsueh B, Jia X, Pasca AM, Bernstein JA, Hallmayer J *et al.* Using induced pluripotent stem cells to investigate cardiac phenotypes in Timothy syndrome. *Nature* 2011;**471**:230–234.
13. Matsa E, Rajamohan D, Dick E, Young L, Mellor I, Staniforth A *et al.* Drug evaluation in cardiomyocytes derived from human induced pluripotent stem cells carrying a long QT syndrome type 2 mutation. *Eur Heart J* 2011;**32**:952–962.
14. World medical association declaration of Helsinki: recommendations guiding physicians in biomedical research involving human subjects. *Cardiovasc Res* 1997;**35**:2–3.
15. Shimoji K, Yuasa S, Onizuka T, Hattori F, Tanaka T, Hara M *et al.* G-CSF promotes the proliferation of developing cardiomyocytes in vivo and in derivation from ESCs and iPSCs. *Cell Stem Cell* 2010;**6**:227–237.
16. Massaeli H, Guo J, Xu J, Zhang S. Extracellular K+ is a prerequisite for the function and plasma membrane stability of HERG channels. *Circ Res* 2010;**106**: 1072–1082.
17. Ravera S, Aluigi MG, Calzia D, Ramoino P, Morelli A, Panfoli I. Evidence for ectopic aerobic ATP production on C6 glioma cell plasma membrane. *Cell Mol Neurobiol* 2011;**31**:313–321.
18. Zwi L, Caspi O, Arbel G, Huber I, Gepstein A, Park I-H *et al.* Cardiomyocyte differentiation of human induced pluripotent stem cells. *Circulation* 2009;**120**: 1513–1523.
19. Zipes DP, Camm AJ, Borggrefe M, Buxton AE, Chaitman B, Fromer M *et al.* ACC/AHA/ESC 2006 Guidelines for Management of Patients With Ventricular Arrhythmias and the Prevention of Sudden Cardiac Death: A Report of the American College of Cardiology/American Heart Association Task Force and the European Society of Cardiology Committee for Practice Guidelines (writing committee to develop guidelines for management of patients with ventricular arrhythmias and the prevention of sudden cardiac death): developed in collaboration with the European Heart Rhythm Association and the Heart Rhythm Society. *Circulation* 2006;**114**: e385–484.
20. Vyas H, Hejlik J, Ackerman MJ. Epinephrine QT stress testing in the evaluation of congenital long-qt syndrome: diagnostic accuracy of the paradoxical QT response. *Circulation* 2006;**113**:1385–1392.
21. Shimizu W, Noda T, Takaki H, Nagaya N, Satomi K, Kurita T *et al.* Diagnostic value of epinephrine test for genotyping LQT1, LQT2, and LQT3 forms of congenital long QT syndrome. *Heart Rhythm* 2004;**1**:276–283.
22. Napolitano C, Priori SG, Schwartz PJ, Bloise R, Ronchetti E, Nastoli J *et al.* Genetic testing in the long QT syndrome. *JAMA* 2005;**294**:2975–2980.
23. Seki T, Yuasa S, Oda M, Egashira T, Yae K, Kusumoto D *et al.* Generation of induced pluripotent stem cells from human terminally differentiated circulating T cells. *Cell Stem Cell* 2010;**7**:11–14.
24. Sartiani L, Bettiol E, Stillitano F, Mugelli A, Cerbai E, Jaconi ME. Developmental changes in cardiomyocytes differentiated from human embryonic stem cells: a molecular and electrophysiological approach. *Stem Cells* 2007;**25**:1136–1144.
25. Jiang P, Rushing SN, Kong C-w, Fu J, Lieu DK-T, Chan CW *et al.* Electrophysiological properties of human induced pluripotent stem cells. *Am J Physiol Cell Physiol* 2010;**298**: C486–C495.
26. Tanaka T, Tohyama S, Murata M, Nomura F, Kaneko T, Chen H *et al.* *In vitro* pharmacologic testing using human induced pluripotent stem cell-derived cardiomyocytes. *Biochem Biophys Res Commun* 2009;**385**:497–502.
27. Marban E. Cardiac channelopathies. *Nature* 2002;**415**:213–218.
28. Roden DM, Abraham RL. Refining repolarization reserve. *Heart Rhythm* 2011;**8**: 1756–1757.
29. Jost N, Papp JG, Varró A. Slow delayed rectifier potassium current (IKs) and the repolarization reserve. *Ann Noninvas Electrocardiol* 2007;**12**:64–78.
30. Viskin S, Halkin A. Treating the long-QT syndrome in the era of implantable defibrillators. *Circulation* 2009;**119**:204–206.

Downloaded from http://cardiovascres.oxfordjournals.org/ at Shiga University of Medical Science Library on February 5, 2013

31. Carvajal-Vergara X, Sevilla A, D'Souza SL, Ang Y-S, Schaniel C, Lee D-F *et al.* Patient-specific induced pluripotent stem-cell-derived models of LEOPARD syndrome. *Nature* 2010;**465**:808–812.
32. Park I-H, Arora N, Huo H, Maherali N, Ahfeldt T, Shimamura A *et al.* Disease-specific induced pluripotent stem cells. *Cell* 2008;**134**:877–886.
33. Emori T, Antzelevitch C. Cellular basis for complex T waves and arrhythmic activity following combined IKr and IKs block. *J Cardiovasc Electrophysiol* 2001;**12**:1369–1378.
34. Cheung AY, Horvath LM, Grafodatskaya D, Pasceri P, Weksberg R, Hotta A *et al.* Isolation of MECP2-null Rett syndrome patient hiPS cells and isogenic controls through X-chromosome inactivation. *Hum Mol Genet* 2011;**20**: 2103–2115.
35. Soldner F, Laganiere J, Cheng AW, Hockemeyer D, Gao Q, Alagappan R *et al.* Generation of isogenic pluripotent stem cells differing exclusively at two early onset Parkinson point mutations. *Cell* 2011;**146**:318–331.

Downloaded from http://cardiovascres.oxfordjournals.org/ at Shiga University of Medical Science Library on February 5, 2013

Journal of Arrhythmia 29 (2013) 65–70

Contents lists available at SciVerse ScienceDirect

Journal of Arrhythmia

journal homepage: www.elsevier.com/locate/joa

Review

Clinical features of Brugada syndrome

Wataru Shimizu, MD, PhD*,[1]

Department of Cardiovascular Medicine, National Cerebral and Cardiovascular Center, 5-7-1 Fujishiro-dai, Suita, Osaka 565-8565, Japan

ARTICLE INFO

Article history:
Received 24 December 2012
Received in revised form
27 December 2012
Accepted 9 January 2013
Available online 21 March 2013

Keywords:
Brugada syndrome
ST segment
Ventricular fibrillation
Diagnosis
Risk stratification

ABSTRACT

Brugada syndrome is a clinical entity characterized by type-1 (coved) ST-segment elevation in the right precordial electrocardiographic leads (V1–V3) and an aborted sudden cardiac death due to ventricular fibrillation (VF) in the absence of structural heart disease. Since 1992, when Brugada and Brugada reported the first case, numerous studies across the world have characterized the clinical, electrocardiographic, electrophysiologic, and prognostic features of Brugada syndrome. Several multicenter studies also suggested the natural history and proposed the risk stratification for subsequent cardiac events. In this review article, the clinical features of Brugada syndrome will be updated.

© 2013 Japanese Heart Rhythm Society. Published by Elsevier B.V. All rights reserved.

Contents

1. Introduction 65
2. Epidemiology 65
3. Electrocardiographic characteristics 66
4. Diagnostic criteria 66
5. Differential diagnosis 67
6. Acquired form of Brugada syndrome 67
7. Clinical features and natural history 67
8. Risk stratification 68
9. Exercise testing 68
10. Signal-averaged ECG 68
11. Fragmented QRS 69
12. Atrial fibrillation 69
13. Programmed electrical stimulation 69
14. Cardiac imaging 69
15. Head-up tilt testing 69
Conflict of interest 69
Acknowledgments 69
References 69

1. Introduction

Brugada syndrome is characterized by specific ST-segment changes in the right precordial electrocardiographic leads, known as the type-1 or coved-type Brugada electrocardiogram (ECG). In addition, Brugada syndrome is associated with a high risk of sudden cardiac death due to ventricular fibrillation (VF) without structural heart diseases. Since Brugada and Brugada first described 8 patients with a history of aborted sudden cardiac death due to VF and type-1 ECG in 1992, Brugada syndrome has become a distinct clinical entity [1–8].

2. Epidemiology

The worldwide prevalence of Brugada syndrome [8] is estimated to be 1 in 10,000, but it is much higher in Asian and

*Tel.: +81 6 6833 5012; fax: +81 6 6872 7486.
E-mail address: wshimizu@hsp.ncvc.go.jp
[1] Current address: Department of Internal Medicine, Division of Cardiology, Nippon Medical School, 1-1-5 Sendagi, Bunkyo-ku, Tokyo 113-8603, Japan.

1880-4276/$ - see front matter © 2013 Japanese Heart Rhythm Society. Published by Elsevier B.V. All rights reserved.
http://dx.doi.org/10.1016/j.joa.2013.01.009

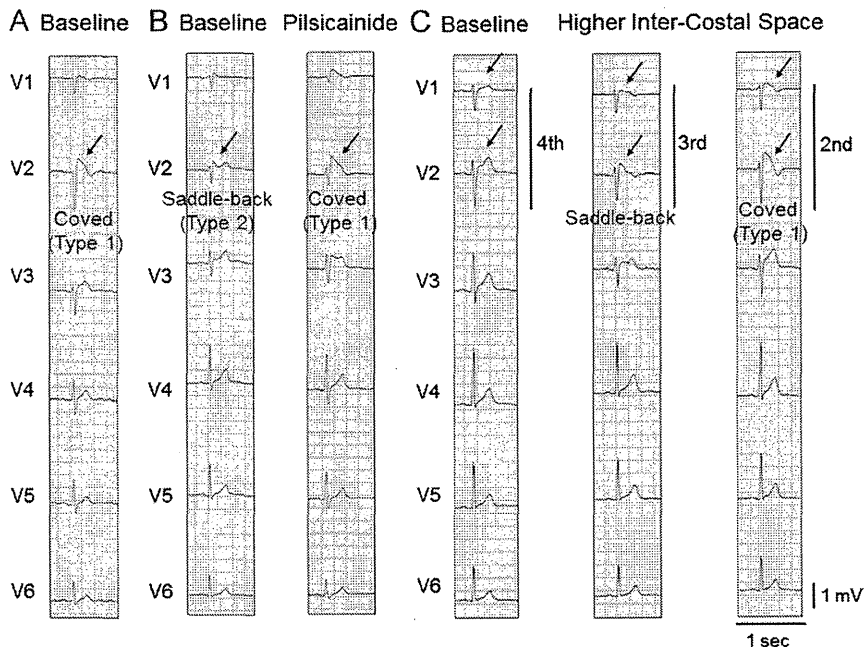

Fig. 1. (A) Spontaneous type-1 (coved) ST-segment elevation (arrow). (B) Unmasking of ST-segment elevation by a class IC sodium channel blocker, pilsicainide. Under baseline condition, type-2 (saddle-back) ST-segment elevation is recorded in lead V2 (left, arrow). Pilsicainide injection (30 mg) unmasks type-1 electrocardiogram (ECG) in lead V2 (right, arrow). (C) Unmasking of type-1 ECG by recordings of right precordial (V1–V2) leads at third and second intercostal spaces. No significant ST-segment elevation is observed in leads V1 and V2 of the standard 12-lead ECG (fourth intercostal space) (left, arrow), while type-2 (middle, arrow) and type-1 (right, arrow) ST-segment elevation are unmasked in leads V1 and V2 recorded from the third and second intercostal spaces, respectively.

Southeast Asian countries, especially Japan, the Philippines, and Thailand, reaching 5–10 in 10,000, while it is much lower in some Eastern European countries like Denmark, with an estimated prevalence of 1.1 in 100,000. Brugada syndrome, also known as pokkuri (Japan), bangungot (the Philippines), and lai tai (Thailand), seems to be the most common cause of natural death in Asian men younger than 50 years. The reason for this higher prevalence in Asia may be in part related to an Asian-specific sequence in the promoter region of *SCN5A* [9].

Brugada syndrome usually manifests during adulthood, with a mean age of sudden death of 41 ± 15 years; however, cases in children are rare [8]. A family history of unexplained sudden death is present in 20–40% of cases in Western countries and 15–20% of cases in Japan [5,8,10,11].

Male predominance in patients with Brugada syndrome is also well known. Since all of the mutations identified in patients with Brugada syndrome display an autosomal dominant mode of transmission, men and women are genetically expected to equally inherit the defective gene. However, the clinical phenotype is 8–10 times more prevalent in men than in women [8]. Experimental studies in dogs have suggested that the presence of a more prominent transient outward current (I_{to}) in males may contribute to the male predominance of the syndrome [12]. Some clinical studies have suggested that higher testosterone levels in men than in women may also have a significant role in the male predominance [13].

Episodes of VF occur more frequently at night or during sleep (2000–0800) than during the daytime as a form of sudden unexplained nocturnal death, syncope, or agonal respiration in approximately 70–80% of patients with Brugada syndrome [8,14,15]. Some authors speculate that this circadian pattern is related to increased vagal tone [16]. Our data detected by implantable cardioverter defibrillator (ICD) have shown that about half of the VF episodes are preceded by ventricular premature complex (VPC) with a similar morphology to initiating VPC of VF [15]. Atrial fibrillation is associated with 10–20% of Brugada cases in Western countries and 20–30% of Brugada cases in Japan [17]. The association of atrioventricular nodal reentrant tachycardia or Wolff-Parkinson-White (WPW) syndrome has also been reported.[18]

3. Electrocardiographic characteristics

The fist Brugada Consensus Report in 2002 suggested 3 types of ST-segment elevation patterns in the right precordial leads of the ECG (Fig. 1) [6]. Type-1 or coved-type ST-segment elevation is characterized by a J-point elevation of ≥ 2 mm (0.2 mV) followed by a negative or isoelectric T-wave (Fig. 1A). Type-2 ST-segment elevation shows a saddleback appearance with a J-point elevation of ≥ 2 mm followed by a trough displaying a ≥ 1-mm ST elevation with either a positive or biphasic T-wave (Fig. 1B). Type-3 ST-segment elevation has a saddleback appearance with a J-point elevation of < 1 mm. The morphology and level of the ST-segment elevation are often accentuated; however, the type-1 or coved-type Brugada ECG is more frequently recognized just before and after episodes of VF [19,20] and is linked to a higher incidence of VF and sudden cardiac death [21]. Although the original report by Brugada and Brugada described the presence of right bundle branch block (RBBB), the RBBB was revealed to be nonessential for the diagnosis of Brugada syndrome [6]. Mild depolarization abnormalities, such as widening of the P wave and QRS duration, and prolongation of the PQ interval are observed in patients with Brugada syndrome, more often in those with *SCN5A* mutations than in those without *SCN5A* mutations [22].

4. Diagnostic criteria

Brugada syndrome is definitively diagnosed when a type-1 ST-segment elevation is observed in at least 1 right precordial lead

(V1 and V2) [23], placed in a standard or a superior position (up to the second intercostal space) (Fig. 1C) [24,25], in the presence or absence of a sodium channel blocking agent (ajmaline, flecainide, pilsicainide, or procainamide) (Fig. 1B). Although the diagnostic criteria from the Second Consensus Report in 2005 require a type-1 ECG in at least 2 right precordial leads (V1–V3) for the definitive diagnosis, several clinical studies thereafter have indicated that a type-1 ECG recorded in at least 1 right precordial lead (V1 and V2) was enough for definitively diagnosing Brugada syndrome [26].

5. Differential diagnosis

Diseases and conditions that can lead to Brugada-like ECG abnormality should be differentially diagnosed. These diseases and conditions include atypical RBBB, left ventricular hypertrophy, early repolarization, acute pericarditis, acute myocardial ischemia or infarction, pulmonary embolism, Prinzmetal angina, dissecting aortic aneurysm, various central and autonomic nervous system abnormalities, Duchenne muscular dystrophy, thiamin deficiency, arrhythmogenic right ventricular cardiomyopathy (ARVC), pectus excavatum, and mechanical compression of the right ventricular outflow tract as occurs in mediastinal tumor or hemopericardium [8,23,27].

6. Acquired form of Brugada syndrome

The ST segment in the right precordial leads is well known to be modulated by several drugs (mainly antiarrhythmic drugs) and autonomic agents [20]. Class IC antiarrhythmic drugs amplify or unmask the ST-segment elevation most effectively as a result of their strong effect of blocking fast sodium current (I_{Na}) [28,29] and are used as a diagnostic tool in latent Brugada syndrome. Many drugs and conditions that increase outward currents (e.g., I_{to}, adenosine triphosphate sensitive potassium current [$I_{K\text{-}ATP}$]) or decrease inward currents (e.g., L-type calcium current [$I_{Ca\text{-}L}$], fast I_{Na}) at the end of phase 1 of the action potential can accentuate or unmask ST-segment elevation, similar to that found in Brugada syndrome (Table 1). This is described as an "acquired" form of Brugada syndrome similar to the "acquired" form of long QT syndrome. Several drugs and conditions other than class IC antiarrhythmic drugs have been reported to produce an acquired form of Brugada syndrome. These drugs and conditions include antianginal drugs; psychotropic drugs; histaminic H1 receptor antagonists; anti-inflammatory drugs; psychoactive recreational drugs; antipsychotic drugs; local anesthetics; short-acting hypnotic agents; hypertestosteronemia; hyperthermia (febrile state); hypothermia; and electrolyte abnormalities, such as hyperkalemia, hypokalemia, hypercalcemia, or hyponatremia [27,30,31]. These drugs and conditions unmask Brugada phenotype mainly by depressing fast I_{Na} and $I_{Ca\text{-}L}$. (See also www.brugadadrugs.org.)

7. Clinical features and natural history

Several symptoms related to Brugada syndrome include (1) VF or aborted sudden cardiac death (more frequent at night than during the day), (2) syncope, (3) nocturnal agonal respiration, (4) palpitations, and (5) chest discomfort. These symptoms are documented frequently at rest, during sleep, or under other vagotonic conditions, but rarely during exercise.

Identification of patients at high risk for sudden cardiac death due to VF is important for managing patients with Brugada syndrome [5,7,10,11,32,33]. Brugada et al. reported that patients with type-1 Brugada ECG initially presenting with aborted sudden cardiac death or VF are at the highest risk for a recurrence (69% at 54 ± 54 months of follow up) [7]. Patients presenting with syncope and a type-1 ECG are also reported to have a high recurrence rate (19% at 26 ± 36 months of follow-up). Even in asymptomatic Brugada patients, a relatively high cardiac-event rate (8%) was reported in their registry. In contrast to the Brugada registry, a recent European registry found a lower incidence of subsequent arrhythmic events. The FINGER study by Probst et al. reported that the annual rates of subsequent or new arrhythmic events in patients with prior aborted sudden cardiac death, patients with prior syncope, and asymptomatic patients are

Table 1
Acquired form of Brugada Syndrome.

1. Antiarrhythmic drugs
(1) Sodium channel blockers
Class IC drugs (Flecainide, Pilsicainide, Propafenone)
Class IA drugs (Ajmaline, Procainamide, Disopyramide, Cibenzoline)
(2) Calcium channel blockers
Verapamil
(3) β blockers
Propranolol, etc.
2. Antianginal drugs
(1) Calcium channel blockers
Nifedipine, Diltiazem, etc.
(2) Nitrate
Isosorbide dinitrate, Nitroglycerine, etc.
(3) Potassium channel openers
Nicorandil, etc.
3. Psychotropic drugs
(1) Tricyclic antidepressants
Amitriptyline, Nortriptyline, Desipramine, Clomipramine, dosulepin, etc.
(2) Tetracyclic antidepressants
Maprotiline, etc.
(3) Phenothiazine
Perphenazine, Cyamemazine, etc.
(4) Benzodiazepine
Clonazepam, Alprazolam, Lorazepam, etc.
(5) Selective serotonin reuptake inhibitors
Fluoxetine, Paroxetine, etc.
(6) Other antidepressants
Trazodone, Risperidone, etc.
4. Other drugs
(1) Histaminic H1 receptor antagonists
Dimenhydrinate, etc.
(2) Anti-inflammatory drugs
Mesalazine, etc.
(3) Psychoactive recreational drugs
Cocaine, Cannabis
(4) Antipsychotic drugs
Lithium, Thioridazine
(5) Local anesthetics
Bupivacaine
(6) Short-acting hypnotic agents
Propofol
5. Hypertestosteronemia
6. Low visceral fat
7. Myocardial ischemia
(1) Right ventricular infarction/ischemia
(2) Vasospastic angina
8. Myocarditis, Pericarditis
(1) Acute myocarditis
(2) Chronic myocarditis
(3) Acute Pericarditis
9. Temperature
(1) Hyperthermia (Febrile state)
(2) Hypothermia
10. Electrolyte abnormalities
(1) Hyperkalemia
(2) Hypokalemia
(3) Hypercalcemia
(4) Hyponatremia
11. Meal, Increased insulin level
12. Polymorphisms in *SCN5A*

7.7%, 1.9%, and 0.5%, respectively [32]. Our Japanese registry endorsed by the Japanese Ministry of Health, Labour and Welfare also demonstrated a lower rate of arrhythmic events than those of the Brugada registry. The annual rate of arrhythmic events in probands with type-1 Brugada ECG was 10.2% in the VF group, 0.6% in the syncope group, and 0.5% in the asymptomatic group [33]. The discrepancy in clinical outcomes of patients between the Brugada registry and the other 2 registries is most likely due to inclusion of particular families with a very severe form of the disease in the Brugada registry.

It is generally agreed that a previous history of aborted cardiac arrest, syncope, presence of a spontaneous type-1 ECG, and male gender are significant predictors of further arrhythmic events [5,7,10,11,32,33].

8. Risk stratification

Considering the natural history of Brugada patients, there is little controversy on the indication of ICD in Brugada patients with a history of aborted cardiac arrest or those with a history of syncope likely caused by VF as class I or class IIa ICD indication. The more important goal is to stratify risk in asymptomatic patients with Brugada syndrome displaying a typical type-1 ECG. Several clinical examinations have been useful in supporting the diagnosis of Brugada syndrome and stratifying high-risk patients.

9. Exercise testing

Some clinical studies have reported the augmentation of ST-segment elevation and/or unmasking of type-1 ECG in the right precordial leads at early recovery periods after exercise in some patients with Brugada syndrome (Fig. 2) [34,35]. We recently investigated the prevalence and the clinical significance of the augmentation of ST-segment elevation at the early recovery phase for risk stratification in Brugada patients [35]. Treadmill exercise testing was conducted in 93 patients with Brugada syndrome (22 documented VF, 35 syncope alone, and 36 asymptomatic) and 102 healthy control subjects. Augmentation of ST-segment elevation ≥ 0.05 mV in leads V1 through V3 compared with baseline was observed at early recovery (1–4 min at recovery) in 34 Brugada patients (37%) (Fig. 2A and B) but not in the remaining 59 Brugada patients (63%) (Fig. 2C) or 102 control subjects. The ST-segment elevation was usually ameliorated at peak exercise (Fig. 2A), but it was augmented even at peak exercise in some patients (Fig. 2B). The Brugada patients associated with the ST-segment augmentation at the early recovery phase had a greater risk of subsequent VF than those without (15/34 [44%] vs. 10/59 [17%], $P=0.004$) during 76 ± 38 months of follow up. Multivariate Cox regression analysis showed that augmentation of ST-segment elevation at the early recovery phase was a significant and independent predictor for cardiac events ($P=0.007$), especially in patients with a history of syncope alone (6/12 [50%] vs. 3/23 [13%]) and in asymptomatic patients (3/15 [20%] vs. 0/21 [0%]). Thus, augmentation of ST-segment elevation at the early recovery phase during exercise testing was specific in patients with Brugada syndrome and can be a predictor of poor prognosis, especially in patients with syncope alone and in asymptomatic patients.

10. Signal-averaged ECG

Frequency of late potentials (LP) in the signal-averaged ECG has been reported to be higher in patients with Brugada syndrome than in control subjects. In a single-center study, Ikeda et al. reported a sensitivity of 89%, specificity of 50%, positive

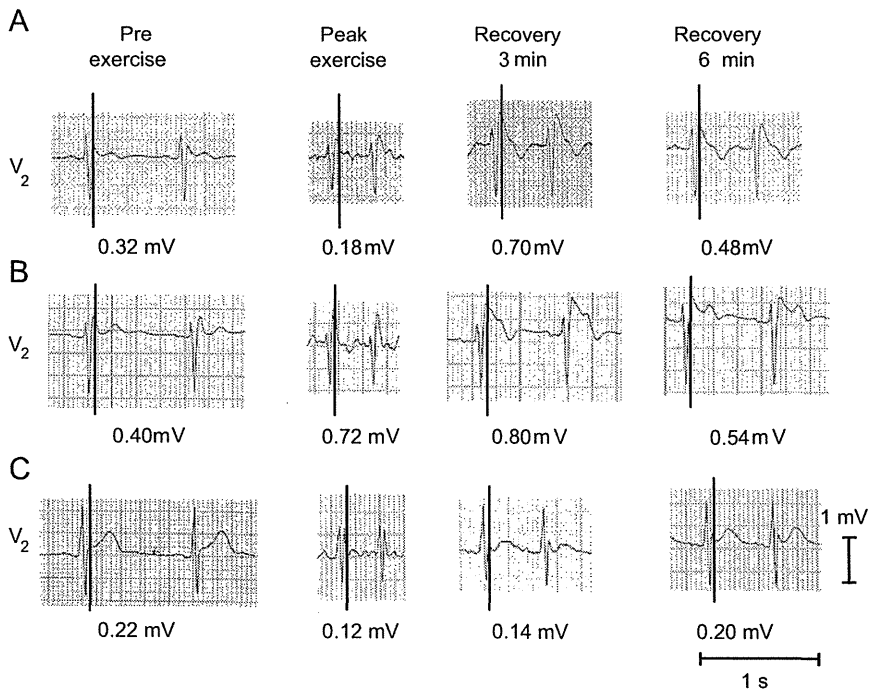

Fig. 2. Responses of ST-segment elevation in lead V2 during exercise testing in 3 patients with Brugada syndrome. (A). The ST-segment elevation was decreased at peak exercise but re-ascended at the early recovery phase (3 min) resulting in typical type-1 ST-segment elevation. (B). In some cases, the ST-segment elevation was augmented at peak exercise and remained augmented at the early recovery phase. (C). The ST-segment elevation was decreased at peak exercise and gradually recovered to the baseline at recovery phase. ST-segment amplitudes are shown as numeric values.

predictive value of 70%, and negative predictive value of 77% for LP for risk stratification of life-threatening events [36].

11. Fragmented QRS

Morita and colleagues reported that fragmented QRS recorded in the standard 12-lead ECGs (with 0- to 150-Hz filters) was more often observed in Brugada patients with VF episodes than in those with syncope or in asymptomatic patients [37]. They also reported that patients who had fragmented QRS frequently experienced recurrence of syncope due to VF within 4 years of the first episode of syncope or VF. More recently, in the PRELUDE study, Priori et al. reported that fragmented QRS was an independent predictor for arrhythmic events in Brugada patients without a history of VF [38].

12. Atrial fibrillation

Spontaneous atrial fibrillation (AF) has been reported to appear in 10–53% of patients with Brugada syndrome and to be associated with a higher incidence of syncopal episodes (60.0% vs. 22.2%, $P < 0.03$) and documented VF (40.0% vs. 14.3%, $P < 0.05$) [39,40].

13. Programmed electrical stimulation

The usefulness of programmed electrical stimulation (PES) to stratify risk of subsequent arrhythmic events has long been controversial between the Brugada registry and other registries [5,7,10,11,32,33]. To fill this gap, Priori organized a multicenter prospective registry (PRELUDE study) with a uniform protocol in patients with Brugada syndrome without a history of VF [38]. They suggested that arrhythmia inducibility during PES was not a predictor of subsequent events during follow-up but that a ventricular effective refractory period < 200 ms was an independent predictor for arrhythmic events. Makimoto et al. recently reported a significance of the number of extrastimuli at PES as a predictor of arrhythmic events in patients with type-1 Brugada ECG [41]. Multivariate Cox regression demonstrated that the induction of VF with up to double extrastimuli was an independent predictor. Therefore, they suggested that up to double extrastimuli were adequate at PES to stratify risk in patients with Brugada syndrome.

14. Cardiac imaging

Several cardiac imaging techniques, such as exercise radionuclide imaging (RI), computed tomography (CT), magnetic resonance imaging (MRI), or echography, are required to prove the absence of structural heart disease, including myocardial ischemia and ARVC.

15. Head-up tilt testing

Head-up tilt (HUT) testing is recommended to judge an episode of syncope to be likely caused by VF by excluding neurally mediated syncope (NMS). However, NMS may coexist with Brugada syndrome [42]. We conducted HUT testing in 46 patients with type-1 Brugada ECG, 20 healthy control subjects, and 15 patients with suspected NMS [43]. HUT testing was positive in 35% of Brugada patients (16/46), 10% of control subjects (2/20), and 67% of suspected NMS patients (10/15). The HUT-positive rate was significantly higher in Brugada patients with VF (7/14; 50%) than that in control subjects (10%) ($P < 0.05$). Augmentation of ST-segment amplitude (≥ 0.05 mV) in leads V1 through V3 was observed in 69% of the HUT-positive Brugada patients (11/16) during vasovagal responses and was associated with augmentation of parasympathetic tone following sympathetic withdrawal, which was evaluated by the heart rate variability. These data suggested that some Brugada patients have an impaired balance of the autonomic nervous system, which may relate to their syncopal episodes.

Conflict of interest

The author have no conflicts of interest to disclose.

Acknowledgments

Dr. Shimizu was supported in part by the Research Grant for the Cardiovascular Diseases (H24-033) from the Ministry of Health, Labour and Welfare, Japan.

References

[1] Brugada P, Brugada J. Right bundle branch block, persistent ST segment elevation and sudden cardiac death: a distinct clinical and electrocardiographic syndrome: a multicenter report. J Am Coll Cardiol 1992;20:1391–6.
[2] Brugada J, Brugada R, Brugada P. Right bundle-branch block and ST-segment elevation in leads V_1 through V_3. A marker for sudden death in patients without demonstrable structural heart disease. Circulation 1998;97:457–60.
[3] Alings M, Wilde A. Brugada syndrome: clinical data and suggested pathophysiological mechanism. Circulation 1999;99:666–73.
[4] Antzelevitch C, Brugada P, Brugada J, et al. Brugada syndrome. A decade of progress. Circ Res 2002;91:1114–8.
[5] Priori SG, Napolitano C, Gasparini M, et al. Natural history of Brugada syndrome: insights for risk stratification and management. Circulation 2002;105:1342–7.
[6] Wilde AA, Antzelevitch C, Borggrefe M, et al. Proposed diagnostic criteria for the Brugada syndrome: consensus report. Circulation 2002;106:2514–9.
[7] Brugada J, Brugada R, Antzelevitch C, et al. Long-term follow-up of individuals with the electrocardiographic pattern of right bundle-branch block and ST-segment elevation in precordial leads V1 to V3. Circulation 2002;105:73–8.
[8] Antzelevitch C, Brugada P, Borggrefe M, et al. Brugada syndrome. Report of the second consensus conference. Endorsed by the Heart Rhythm Society and the European Heart Rhythm Association. Circulation 2005;111:659–70.
[9] Bezzina CR, Shimizu W, Yang P, et al. A common sodium channel promoter haplotype in Asian subjects underlies variability in cardiac conduction. Circulation 2006;113:338–44.
[10] Kanda M, Shimizu W, Matsuo K, et al. Electrophysiologic characteristics and implication of induced ventricular fibrillation in symptomatic patients with Brugada syndrome. J Am Coll Cardiol 2002;39:1799–805.
[11] Eckardt L, Probst V, Smits JP, et al. Long-term prognosis of individuals with right precordial ST-segment-elevation Brugada syndrome. Circulation 2005;111:257–63.
[12] Di Diego JM, Cordeiro JM, Goodrow RJ, et al. Ionic and cellular basis for the predominance of the Brugada syndrome phenotype in males. Circulation 2002;106:2004–11.
[13] Shimizu W, Matsuo K, Kokubo Y, et al. Sex hormone and gender difference. Role of testosterone on male predominance in Brugada syndrome. J Cardiovasc Electrophysiol 2007;18:415–21.
[14] Matsuo K, Kurita T, Inagaki M, et al. The circadian pattern of the development of ventricular fibrillation in patients with Brugada syndrome. Eur Heart J 1999;20:465–70.
[15] Takigawa M, Noda T, Shimizu W, et al. Seasonal and circadian distributions of ventricular fibrillation in patients with Brugada syndrome. Heart Rhythm 2008;5:1523–7.
[16] Mizumaki K, Fujiki A, Tsuneda T, et al. Vagal activity modulates spontaneous augmentation of ST elevation in the daily life of patients with Brugada syndrome. J Cardiovasc Electrophysiol 2004;15:667–73.
[17] Morita H, Kusano-Fukushima K, Nagase S, et al. Atrial fibrillation and atrial vulnerability in patients with Brugada syndrome. J Am Coll Cardiol 2002;40:1437–44.
[18] Eckardt L, Kirchhof P, Johna R, et al. Wolff-Parkinson-White syndrome associated with Brugada syndrome. Pacing Clin Electrophysiol 2001;24:1423–4.
[19] Matsuo K, Shimizu W, Kurita T, et al. Dynamic changes of 12-lead electrocardiograms in a patient with Brugada syndrome. J Cardiovasc Electrophysiol 1998;9:508–12.

[20] Miyazaki T, Mitamura H, Miyoshi S, et al. Autonomic and antiarrhythmic drug modulation of ST segment elevation in patients with Brugada syndrome. J Am Coll Cardiol 1996;27:1061–70.
[21] Atarashi H, Ogawa S, Harumi K, et al. Idiopathic Ventricular Fibrillation Investigators: three-year follow-up of patients with right bundle branch block and ST segment elevation in the right precordial leads: Japanese Registry of Brugada Syndrome. Idiopathic Ventricular Fibrillation Investigators. J Am Coll Cardiol 2001;37:1916–20.
[22] Smits JP, Eckardt L, Probst V, et al. Genotype-phenotype relationship in Brugada syndrome: electrocardiographic features differentiate SCN5A-related patients from non-SCN5A-related patients. J Am Coll Cardiol 2002;40:350–6.
[23] Priori SG, Wilde A, Horie M, et al. HRS/EHRA/APHRS expert consensus statement on the management of inherited arrhythmias. This document was developed as a partnership between the Heart Rhythm Society (HRS), the European Heart Rhythm Association (EHRA), and Asian Pacific Heart Rhythm Society (APHRS). Heart Rhythm, submitted for publication.
[24] Miyamoto K, Yokokawa M, Tanaka K, et al. Diagnostic and prognostic value of type 1 Brugada electrocardiogram at higher (third or second) V1 to V2 recording in men with Brugada syndrome. Am J Cardiol 2007;99:53–7.
[25] Nagase S, Hiramatsu S, Morita H, et al. Electroanatomical correlation of repolarization abnormalities in Brugada syndrome: detection of type 1 electrocardiogram in the right ventricular outflow tract. J Am Coll Cardiol 2010;56:2143–5.
[26] Sarkozy A, Sorgente A, Boussy T, et al. The value of a family history of sudden death in patients with diagnostic type I Brugada ECG pattern. Eur Heart J 2011;32:2153–60.
[27] Shimizu W. Acquired forms of the Brugada syndrome. J Electrocardiol 2005;38:22–5.
[28] Shimizu W, Antzelevitch C, Suyama K, et al. Effect of sodium channel blockers on ST segment, QRS duration, and corrected QT interval in patients with Brugada syndrome. J Cardiovasc Electrophysiol 2000;11:1320–9.
[29] Brugada R, Brugada J, Antzelevitch C, et al. Sodium channel blockers identify risk for sudden death in patients with ST-segment elevation and right bundle branch block but structurally normal hearts. Circulation 2000;101:510–5.
[30] Baranchuk A, Nguyen T, Ryu MH, et al. Brugada phenocopy: new terminology and proposed classification. Ann Noninvasive Electrocardiol 2012;17:299–314.
[31] Shimizu W. Acquired form of Brugada syndrome: Chapter 40, . In: Gussak I, Antzelevitch C, Wilde A, Powell B, Ackerman MJ, Shen WK, editors. Electrical diseases of the heart (second edition): genetics, mechanisms, treatment, prevention, Part III. Secondary hereditary and acquired cardiac channelopathies, and sudden cardiac death. UK, Springer, in press.
[32] Probst V, Veltmann C, Eckardt L, et al. Long-term prognosis of patients diagnosed with Brugada syndrome: results from the FINGER Brugada Syndrome Registry. Circulation 2010;121:635–43.
[33] Kamakura S, Ohe T, Nakazawa K, et al. Long-term prognosis of probands with Brugada-pattern ST-elevation in leads V1-V3. Circ Arrhythm Electrophysiol 2009;2:495–503.
[34] Amin AS, de Groot EA, Ruijter JM, et al. Exercise-induced ECG changes in Brugada 1328 syndrome. Circ Arrhythm Electrophysiol 2009;2:531–9.
[35] Makimoto H, Nakagawa E, Takaki H, et al. Augmented ST-segment elevation during recovery from exercise predicts cardiac events in patients with Brugada syndrome. J Am Coll Cardiol 2010;56:1576–84.
[36] Ikeda T, Sakurada H, Sakabe K, et al. Assessment of noninvasive markers in identifying patients at risk in the Brugada syndrome: insight into risk stratification. J Am Coll Cardiol 2001;37:16–34.
[37] Morita H, Kusano KF, Miura D, et al. Fragmented QRS as a marker of conduction abnormality and a predictor of prognosis of Brugada syndrome. Circulation 2008;118:1697–704.
[38] Priori SG, Gasparini M, Napolitano C, et al. Risk stratification in Brugada syndrome: results of the PRELUDE (PRogrammed ELectrical stimUlation preDictive valuE) registry. J Am Coll Cardiol 2012;59:37–45.
[39] Morita H, Kusano KF, Nagase S, et al. Atrial fibrillation and atrial vulnerability in patients with Brugada syndrome. J Am Coll Cardiol 2002;40:1437–44.
[40] Kusano KF, Taniyama M, Nakamura K, et al. Atrial fibrillation in patients with Brugada syndrome relationships of gene mutation, electrophysiology, and clinical backgrounds. J Am Coll Cardiol 2008;51:1169–75.
[41] Makimoto H, Kamakura S, Aihara N, et al. Clinical impact of the number of extrastimuli in programmed electrical stimulation in patients with Brugada type 1 electrocardiogram. Heart Rhythm 2012;9:242–8.
[42] Márquez MF, Rivera J, Hermosillo AG, et al. Arrhythmic storm responsive to quinidine in a patient with Brugada syndrome and vasovagal syncope. Pacing Clin Electrophysiol 2005;28:870–3.
[43] Yokokawa M, Okamura H, Noda T, et al. Neurally-mediated syncope as a cause of syncope in patients with Brugada electrocardiogram. J Cardiovasc Electrophysiol 2010;21:186–92.

Heart Vessels
DOI 10.1007/s00380-012-0235-8

CASE REPORT

A left ventricular noncompaction in a patient with long QT syndrome caused by a *KCNQ1* mutation: a case report

Kentaro Nakashima · Isao Kusakawa · Tsuyoshi Yamamoto · Shinsuke Hirabayashi · Ryohta Hosoya · Wataru Shimizu · Naokata Sumitomo

Received: 29 July 2011 / Accepted: 20 January 2012
© Springer 2012

Abstract A 5-year-old girl developed cardiopulmonary arrest after crying. From the electrocardiogram and echocardiography, a left ventricular noncompaction (LVNC) with long QT syndrome (LQT) was suspected as the cause of the cardiopulmonary arrest, and treatment with a β-blocker and a calcium antagonist was then begun. A genetic screening of LQT-related genes revealed a previously reported heterozygous *KCNQ1* mutation. The association of LVNC and LQT is an extremely rare condition, and long-term treatment based on the characteristics of both disorders is required. Also, the association of cardiomyopathy and LQT could become a new clinical entity in the future.

Keywords Long QT syndrome · Left ventricular noncompaction · Epilepsy · Cardiopulmonary arrest · *KCNQ1* mutation

K. Nakashima · I. Kusakawa · T. Yamamoto · S. Hirabayashi · R. Hosoya
Department of Pediatrics, St. Luke's International Hospital, 9-1 Akashi-cho, Chuou-ku, Tokyo 104-8560, Japan
e-mail: bluesky199067@yahoo.co.jp; nakashima.k@nk-cc.go.jp

Present Address:
K. Nakashima
Department of Pediatrics, National Hospital Organization Kyushu Cancer Center, 3-1-1 Notame, Minami-ku, Fukuoka City, Fukuoka 811-1395, Japan

W. Shimizu
Department of Cardiovascular Medicine, National Cerebral and Cardiovascular Center, 5-7-1 Fujishiro-dai, Suita, Osaka 565-8565, Japan

N. Sumitomo (✉)
Department of Pediatrics and Child Health, Nihon University School of Medicine, 30-1 Oyaguchi Kamimachi, Itabashi-ku, Tokyo 173-8610, Japan
e-mail: sumitomo.naokata@nihon-u.ac.jp

Background

Long QT syndrome (LQT) is a group of ion-channel disorders of the myocardium that may prolong the repolarization of the cardiac cycle [1]. According to the genotype investigation, 12 subtypes (LQT1–12) have been reported [2]; each subtype has its own clinical characteristics, and the treatment strategy differs for each subtype. Long QT syndrome is known as the most important cause of sudden cardiac death in the young [3], and may mostly result from the occurrence of ventricular fibrillation (VF) or torsade de pointes (TdP).

Here we report the case of a girl with left ventricular noncompaction (LVNC) and LQT, which were confirmed after resuscitation from cardiopulmonary arrest.

Case report

A 5-year-old girl had syncope after intense crying at her kindergarten. Her mother noticed cyanosis around her lips and then she developed cardiopulmonary arrest. Bystander cardiopulmonary resuscitation (CPR) was started immediately by a kindergarten teacher, who called for an ambulance. An automated external defibrillator (AED) revealed pulseless electrical activity, and there was no indication for defibrillation. She was transported to our hospital under continuous CPR.

She had been followed up for a diagnosis of epilepsy after two episodes of afebrile convulsions when she was 3 years old. She had a syncopal attack during the follow-up period, and multifocal spike waves were noted on the electroencephalogram. She had been administered carbamazepine since then, after which the spike waves disappeared during the follow-up period. Except for an

Published online: 22 February 2012

episode of afebrile convulsions at age 4 years, she did not experience any further episodes of convulsions or syncope. Magnetic resonance imaging revealed no brain abnormalities.

On arrival at our hospital, sinus rhythm had resumed; however, she required intubation and respiratory support for her respiratory failure and cardiac dysfunction. Her cardiac function then improved gradually, but about 6 h after arrival, TdP and VT emerged in the intensive care unit. While we were preparing to defibrillate her, performing cardiac compressions for about 1 min, sinus rhythm resumed spontaneously (Fig. 1) and her cardiac function improved.

The electrocardiogram obtained after the CPR exhibited a prolonged QTc interval (Fig. 2, QTc = 0.6 s), and the patient was suspected as having LQT. There were no electrolyte imbalances at the time of hospitalization. Her cardiac function improved gradually after CPR. An echocardiogram revealed a spongy dysplastic left ventricular myocardium with prominent trabeculations and deep recesses, indicating LVNC (Fig. 3). We therefore started the patient on propranolol and verapamil to control her VT. Her respiratory support was discontinued 3 days after hospitalization. After administration of propranolol and verapamil, TdT and VT no longer emerged.

Electrocardiographic examinations and a genetic screening of LQT-related genes were performed on the patient, her sister and brother, her parents, her paternal and maternal grandfathers and grandmothers, and a maternal uncle (Fig. 4). She, her brother, her father, and her paternal grandmother were found to have a previously reported heterozygous *KCNQ1* mutation c.1831 G > T in exon 15 (p. D611T). No prolongation of QT intervals or echocardiographic abnormalities were found in family members (her brother, her father, and her paternal grandmother) who had a *KCNQ1* mutation. Although her development had been normal until this event, the patient manifested mild mental retardation because of ischemic brain damage. She underwent rehabilitation and attended a school for handicapped children with a restriction on swimming.

Discussion

Left ventricular noncompaction is a congenital cardiomyopathy with a spongy morphological appearance and deep intertrabecular sinusoids in communication with the ventricular cavity [4]. The diagnosis is mainly made by two-dimensional echocardiography, cardiac magnetic resonance imaging, or left ventricular angiography.

The echocardiogram reveals that prominent trabeculations and deep recesses are noted in the ventricular myocardium [5]. However, so far there has been no distinct definition of LVNC [6]. Koh et al. [7] reported that a left ventricular myocardial deformation is reduced in the longitudinal and circumferential dimensions and manifests with tight systolic–diastolic coupling in children with LVNC.

Genetic mutations were first reported in the *G4.5* gene in patients with an isolated LVNC [8]. Z-line and mitochondrial mutations and X-linked inheritance resulting from mutations in the *G4.5* gene encoding tafazzin could be a pathogenesis for the disease. In this report, the gene defect differed among the families, and thus there did not appear

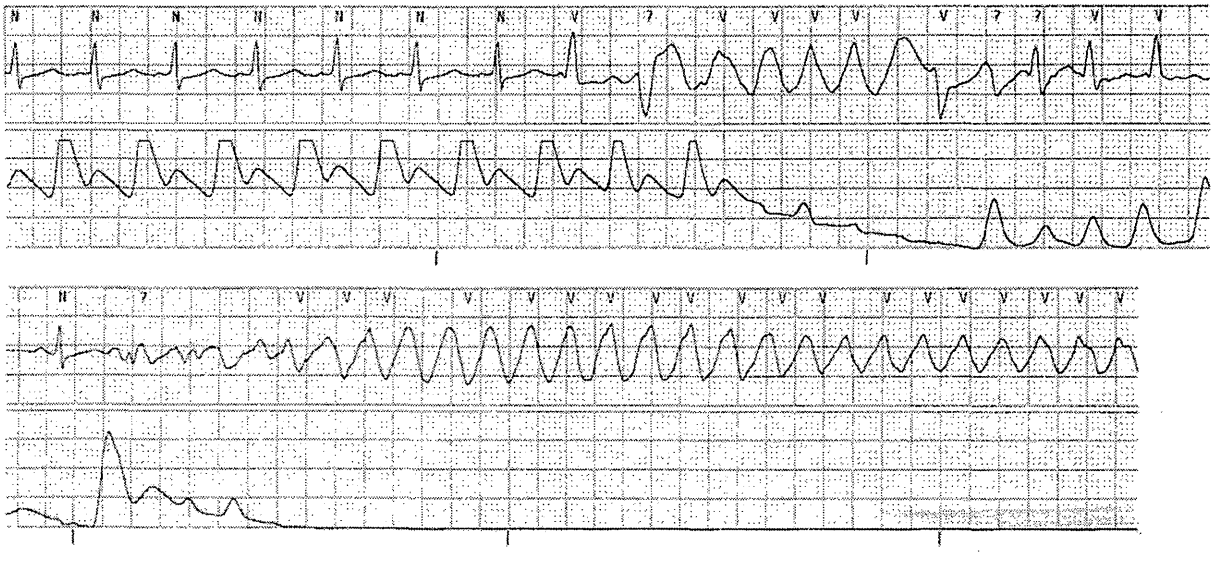

Fig. 1 Monitor recording obtained while the patient was in the intensive care unit. *Upper panel* occurrence of torsade de pointes (TdP), which terminated within several beats. *Lower panel* occurrence of long-lasting TdP or ventricular fibrillation

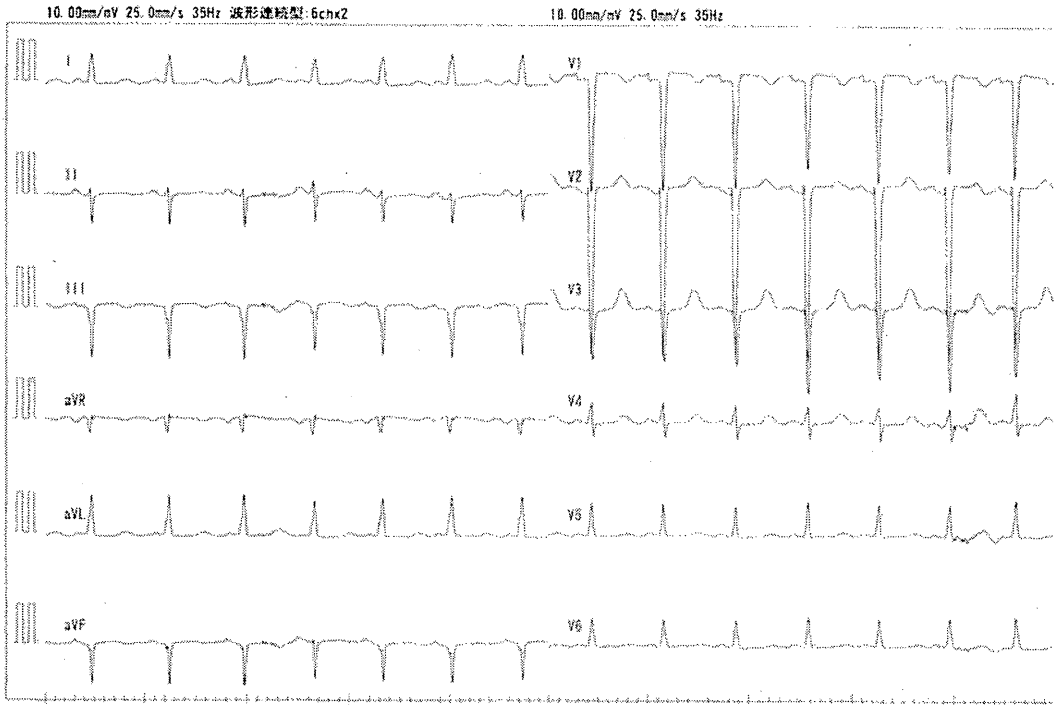

Fig. 2 Electrocardiogram recorded after the resuscitation. The electrocardiogram after the resuscitation showed normal sinus rhythm with left QRS axis deviation (−15°). The QTc interval was prolonged to 0.6 s. There were also flattened T waves in the left precordial leads (V5 and V6)

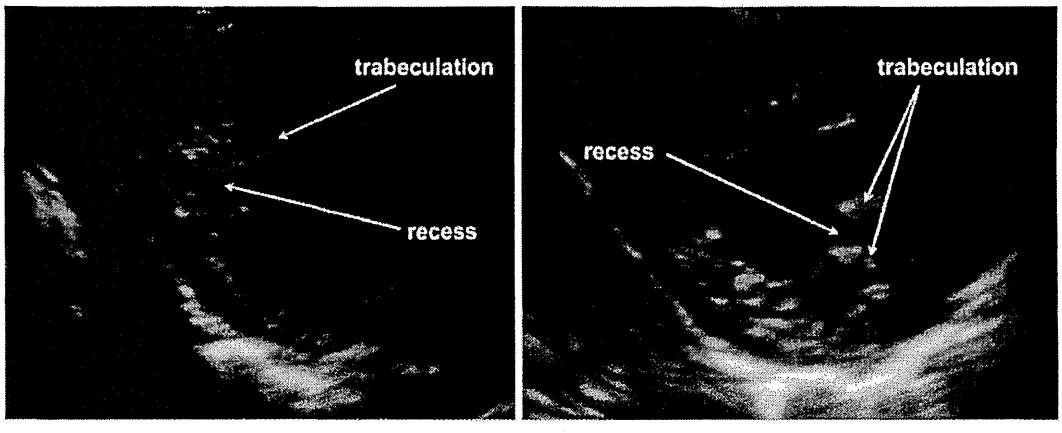

Fig. 3 Echocardiogram. Prominent trabeculations and a deep recess were detected

to be any obvious genotype–phenotype correlation that would allow for the differentiation of the clinical course to be predicted. In addition, the cardiac phenotypes that occur as a result of *G4.5* mutations may vary significantly. On the other hand, in patients with LVNC associated with congenital heart disease, a so-called nonisolated LVNC, mutations in the α-dystrobrevin gene have been reported [9]. In this report, the α-dystrobrevin mutation resulted in a phenotype of a dilated hypertrophic cardiomyopathy with deep trabeculations associated with congenital heart disease, consistent with the criteria for LVNC. However, the phenotype in this family had considerable variability. Consequently, the details of the relation between an ion-channel dysfunction and the maldevelopment of the ventricular myocardium are not well described. Further genetic studies are needed to discover whether a combined mutation with *G4.5* or α-dystrobrevin and *KCNQ1* could have contributed to this clinical manifestation in this patient.

The association of LVNC with LQT is extremely rare. *SCN5A* mutations are frequently associated with LVNC.

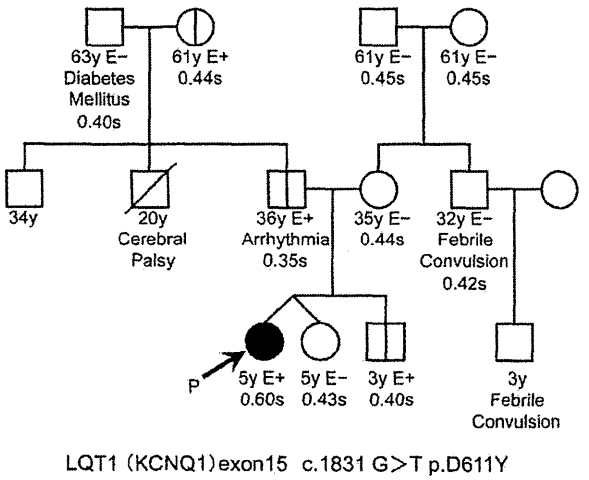

Fig. 4 Family tree of our patient. The *arrow* shows the proband. *KCNQ1* mutations were detected in the proband, and her brother, father, and grandmother

However, only 2 of 62 patients were found to have LQT in *SCN5A*-positive LVNC [10]. *SCN5A* mutations are well known as a cause of LQT3 syndrome and Brugada syndrome. Ogawa et al. [11] reported a *KCNH2* mutation in two patients with LQT and LVNC. *KCNH2* mutations have been known to be the cause of LQT2 syndrome.

KCNQ1 mutations are known as a cause of LQT [12]. However, to the best of our knowledge there have been no previous reports on the association of a *KCNQ1* mutation and LVNC, so this is the first report suggesting an association between LQT1 and LVNC.

The association of cardiomyopathy and LQT could become a new clinical entity in the future. In 2006, the American Heart Association scientific statement on the classification of cardiomyopathies formally classified LVNC as its own disease entity, as a primary cardiomyopathy with a genetic origin, in the same category as ion-channel disorders [13]. Long-term follow-up will be required to reveal further associations between both disorders.

Conclusion

The association of LQT with LVNC is extremely rare. There have been only two patients with *SCN5A* mutations and two patients with *KCNH2* mutations reported to date. This is the first report of a *KCNQ1* mutation with LQT and LVNC. A genetic screening of LQT-related genes is recommended for patients with a long QT interval and LVNC.

Acknowledgments The authors thank Mr. John Martin for his linguistic assistance with this article.

References

1. Moss AJ (2003) Long QT syndrome. JAMA 289:2041–2044
2. Hedley PL, Jørgensen P, Schlamowitz S, Wangari R, Moolman-Smook J, Brink PA, Kanters JK, Corfield VA, Christiansen M (2009) The genetic basis of long QT and short QT syndromes: a mutation update. Hum Mutat 30:1486–1511
3. Li H, Fuentes-Garcia J, Towbin JA (2000) Current concepts in long QT syndrome. Pediatr Cardiol 21:542–550
4. Maron BJ, Towbin JA, Thiene G, Antzelevitch C, Corrado D, Arnett D, Moss AJ, Seidman CE, Young JB (2006) Contemporary definitions and classification of the cardiomyopathies. Circulation 113:1807–1816
5. Jenni R, Oechslin E, Schneider J, Attenhofer Jost C, Kaufmann PA (2001) Echocardiographic and pathoanatomical characteristics of isolated left ventricular non-compaction: a step towards classification as a distinct cardiomyopathy. Heart 86:666–671
6. Chin TK, Perloff JK, Williams RG, Jue K, Mohrmann R (1990) Isolated noncompaction of left ventricular myocardium. A study of eight cases. Circulation 82:507–513
7. Koh C, Hong WJ, Wong SJ, Cheung YF (2010) Systolic–diastolic coupling of myocardial deformation of the left ventricle in children with left ventricular noncompaction. Heart Vessels 25:493–499
8. Bleyl SB, Mumford BR, Thompson V, Carey JC, Pysher TJ, Chin TK, Ward K (1997) Neonatal, lethal noncompaction of the left ventricular myocardium is allelic with Barth syndrome. Am J Hum Genet 61:868–872
9. Ichida F, Tsubata S, Bowles KR, Haneda N, Uese K, Miyawaki T, Dreyer WJ, Messina J, Li H, Bowles NE, Towbin JA (2001) Novel gene mutations in patients with left ventricular noncompaction or Barth syndrome. Circulation 103:1256–1263
10. Shan L, Makita N, Xing Y, Watanabe S, Futatani T, Ye F, Saito K, Ibuki K, Watanabe K, Hirono K, Uese K, Ichida F, Miyawaki T, Origasa H, Bowles NE, Towbin JA (2008) SCN5A variants in Japanese patients with left ventricular noncompaction and arrhythmia. Mol Genet Metab 93:468–474
11. Ogawa K, Nakamura Y, Terano K, Ando T, Hishitani T, Hoshino K (2009) Isolated non-compaction of the ventricular myocardium associated with long QT syndrome: a report of 2 cases. Circ J 73:2169–2172
12. Bokil NJ, Baisden JM, Radford DJ, Summers KM (2010) Molecular genetics of long QT syndrome. Mol Genet Metab 101:1–8
13. Maron BJ, Towbin JA, Thiene G, Antzelevitch C, Corrado D, Arnett D, Moss AJ, Seidman CE, Young JB; American Heart Association; Council on Clinical Cardiology, Heart Failure and Transplantation Committee; Quality of Care and Outcomes Research and Functional Genomics and Translational Biology Interdisciplinary Working Groups; Council on Epidemiology and Prevention (2006) Contemporary definitions and classification of the cardiomyopathies: an American Heart Association Scientific Statement from the Council on Clinical Cardiology, Heart Failure and Transplantation Committee. Circulation 113:1807–1816

ARRHYTHMIA ROUNDS

Section Editor: George J. Klein, M.D.

Double Tachycardia After Slow Pathway Ablation for Atrioventricular Nodal Tachycardia: What Is the Mechanism?

HISAKI MAKIMOTO, M.D., KAZUHIRO SATOMI, M.D., PH.D., MITSURU WADA, M.D., and WATARU SHIMIZU, M.D., PH.D.

From the Division of Arrhythmia and Electrophysiology, Department of Cardiovascular Medicine, National Cerebral and Cardiovascular Center, Suita, Japan

atrioventricular nodal reentrant tachycardia, atrial fibrillation, catheter ablation, double tachycardia

Case Presentation

A healthy 42-year-old man was referred to our hospital for an electrophysiological study of paroxysmal supraventricular tachycardia. The surface 12-lead ECG showed no preexcitation during sinus rhythm and a regular narrow QRS tachycardia at a rate of 200 beats per minute. Sinus node function and atrioventricular nodal (AVN) conduction at baseline were normal. Atrial extra stimulation demonstrated a sudden jump in AV conduction. The clinical tachycardia was reproducibly induced during isoproterenol administration by double atrial extrastimuli (500/360/260 milliseconds) from the HRA. The tachycardia was diagnosed as slow–fast AVNRT based on the existence of dual antegrade AVN pathways, the same atrial activation sequence during the tachycardia and RV pacing, no atrial capture by RV stimulation during the tachycardia, and the result of para-Hisian pacing. Initially, anatomical guided radiofrequency (RF) applications were delivered to the right inferoseptal region (55°C, 30 W). Even

J Cardiovasc Electrophysiol, Vol. 24, pp. 233-236, February 2013.

No disclosures.

Address for correspondence: Kazuhiro Satomi, M.D., Ph.D., Division of Arrhythmia and Electrophysiology, Department of Cardiovascular Medicine, National Cerebral and Cardiovascular Center, 5-7-1 Fujishiro-dai, Suita, Osaka 565-8565, Japan. Fax: 81-6-6872-7486; E-mail: ksatomi@hsp.ncvc.go.jp

doi: 10.1111/jce.12004

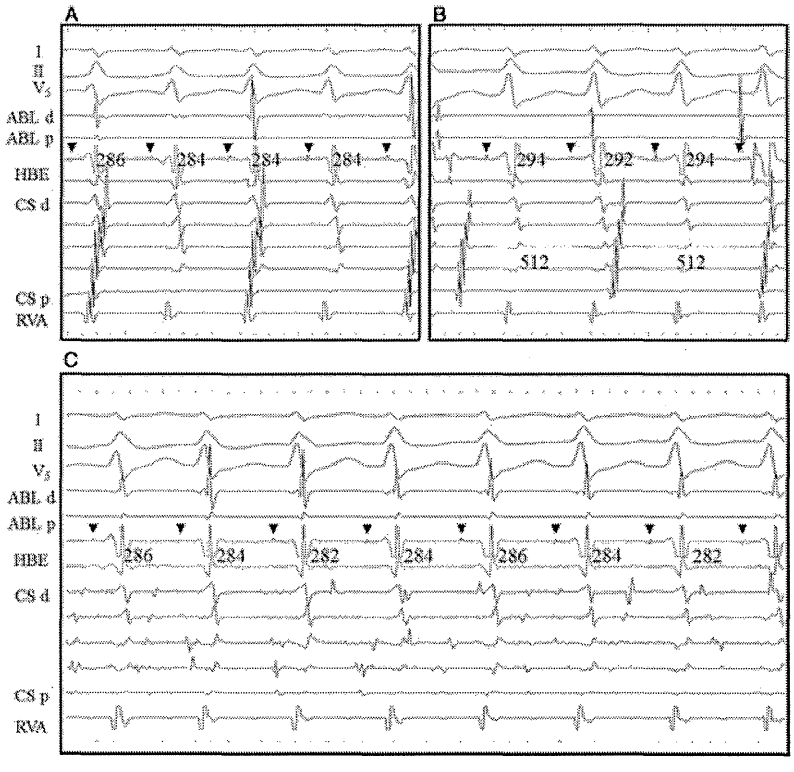

Figure 1. *During the tachycardia (CL 284 milliseconds), 2 to 1 ventriculoatrial block was observed (A). After the atrium returned to sinus rhythm (CL 512 milliseconds), the tachycardia still continued (CL 294 milliseconds) (B). The atrium exhibited atrial fibrillation while the tachycardia persisted (C). The ablation catheter was positioned near the lateral wall of the right atrium. The arrowheads indicate the His deflection. d = distal; p = proximal; ABL = ablation catheter; CL = cycle length; CS = coronary sinus; HA = His-atrium; HBE = His bundle electrode; HRA = high right atrium; RVA = right ventricular apex; SA = stimulus-atrium.*

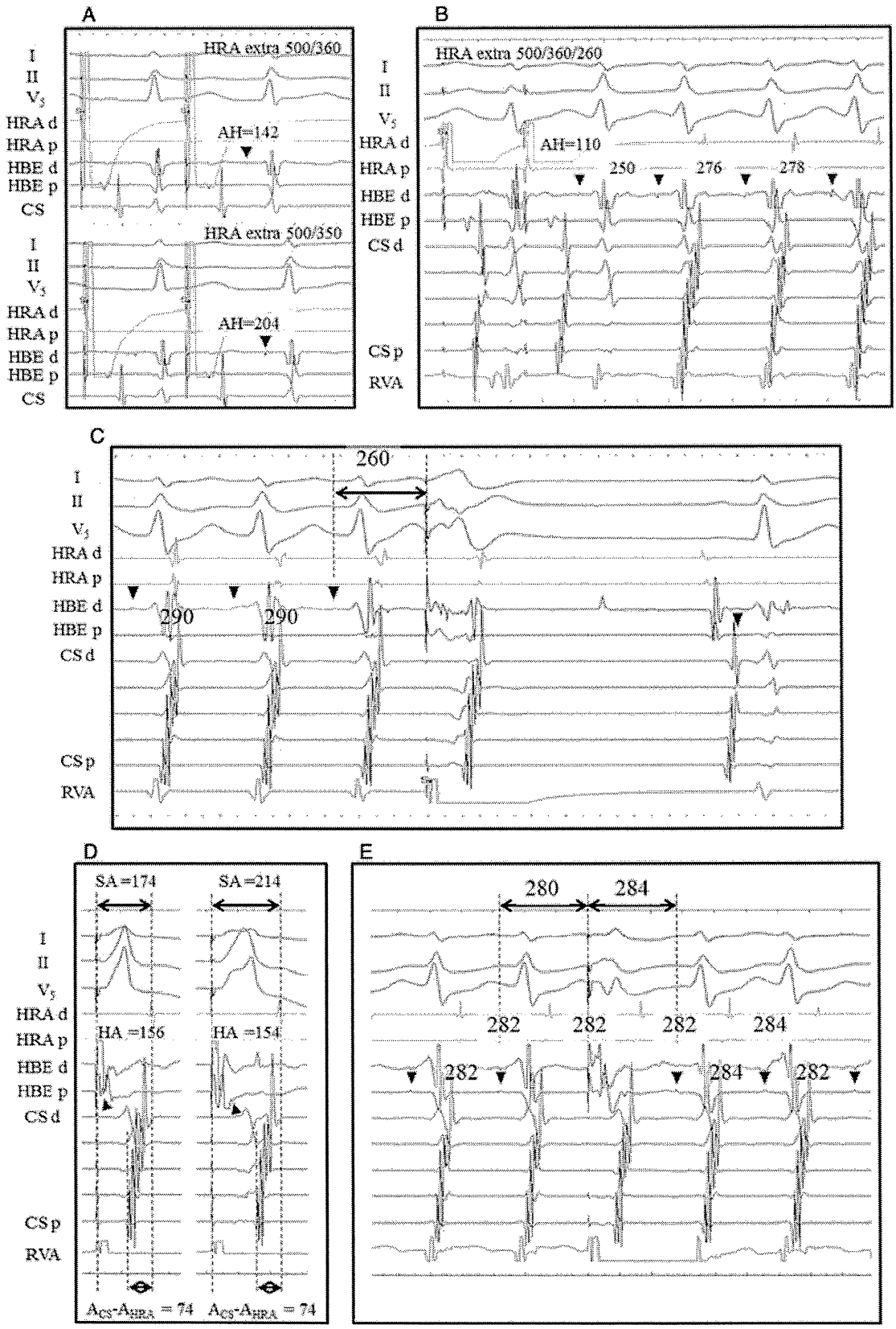

Figure 2. *A sudden jump-up phenomenon of AH interval was observed (A). The double ventricular response was reproducibly observed at the beginning of the tachycardia (B). The tachycardia was terminated by the ventricular extrastimuli (C). Para-Hisian pacing showed that the retrograde conduction was through the atrioventricular node (D). Ventricular extrastimuli during the refractory of His did not proceed the atrial excitation (E). The arrowheads indicate the His deflection. The abbreviations are as in Figure 1.*

after 19 applications with an accelerated junctional rhythm, the tachycardia remained inducible. A 2:1 VA block and dissociated atrial activation were observed during the tachycardia (Fig. 1A,B). Moreover, the tachycardia sustained while AF was induced by atrial pacing (Fig. 1C). What is the mechanism of the double tachycardia, and is the diagnosis of slow–fast AVNRT correct?

Commentary

Despite the advances in cardiac electrophysiology, it remains in debate whether or not the atrium is involved in the circuit of AVNRT. A few case reports have described the persistence of AVNRT despite the occurrence of different VA block patterns indicating the existence of an upper common pathway (UCP) connecting a subatrial (intranodal) reentrant circuit to the atria. To the best of our knowledge, only one case report has described the rare phenomenon of AF and AVNRT being simultaneously sustained in a patient with slow–fast AVNRT, indicating a "double tachycardia."[1]

At the baseline, the effective refractory period (ERP) of the antegrade fast pathway (FP) and slow pathway (SP) was 360 and 340 milliseconds, respectively, following an 8 consecutive beat pacing (cycle length [CL] 500 milliseconds; Fig. 2A). RV pacing exhibited 1:1 VA conduction at pacing intervals over 333 milliseconds. RV extra stimulation demonstrated no jump-up phenomenon, and the ERP of the VA conduction was less than 210 milliseconds when the ventricular refractory period was attained. The reproducible tachycardia induction under an isoproterenol administration by double atrial extrastimuli showed the double ventricular response at the beginning of the tachycardia (Fig. 2B). The tachycardia was terminated by the ventricular extrastimuli and burst pacing (Fig. 2C). Moreover, the same atrial activation sequence during the tachycardia and RV pacing, no atrial capture by RV stimulation during the tachycardia, and the atrial activation sequence during para-Hisian pacing validated the diagnosis as slow–fast AVNRT (Fig. 2D, 2E). After multiple RF applications at the right inferoseptal region (SP area) with an accelerated junctional rhythm, the AVNRT remained still inducible. Furthermore, a regular H–H interval was observed during the sinus rhythm and the AF, suggesting VA and AV block occurred during the tachycardia (Fig. 1). Following administration of a bolus ATP, the AVNRT was terminated after the CL prolonged to 344 milliseconds, although AF persisted (Fig. 3A). After the spontaneous termination of the AF, the antegrade ERP of the FP and SP was 290 and 270 milliseconds, respectively. The retrograde ERP of the FP was 390 milliseconds. Although the antegrade AVN conduction should have been better than that at baseline, the activation during AF could not enter the AVNRT circuit. This could be explained by (1) a very small excitable gap or circuit or (2) functional block in the UCP. The fact that the AVNRT could be entrained from the SP area at relatively longer CL (270 milliseconds), but not from the FP area, was considered to support the existence of functional block (Fig. 3B).

After we performed additional RF applications (40 W, 55°C) in the SP area, the AVNRT became noninducible even under an ISP administration. The ERP of the anterograde FP

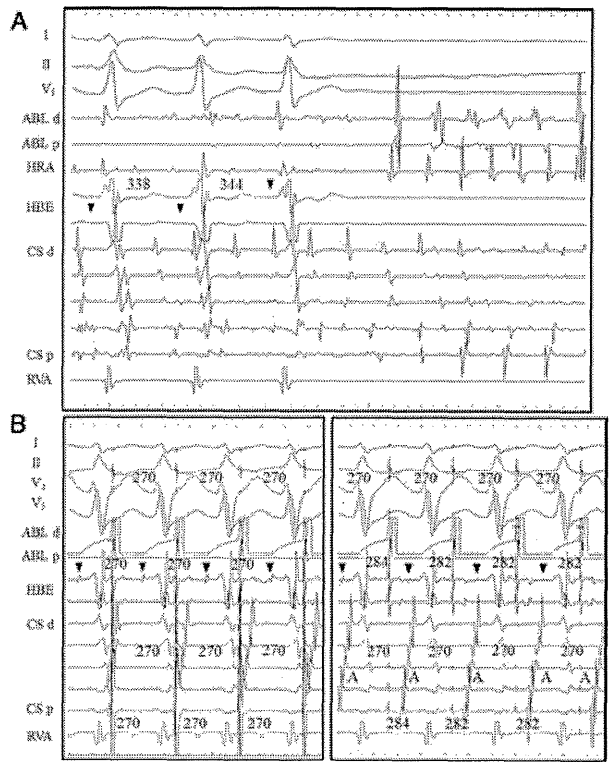

Figure 3. *After a bolus ATP venous administration, the cycle length of the tachycardia prolonged to 344 milliseconds, and the AVNRT was terminated, though AF persisted (A). The AVNRT (CL 282 milliseconds) could be entrained by pacing (CL 270 milliseconds) from the slow pathway area, (B; left panel) but not by pacing from the fast pathway (B; right panel). The arrowheads indicate the His deflection. The abbreviations are as in Figure 1.*

shortened to 270 milliseconds, and the jump phenomenon was no longer observed at the end of the procedure. No complications including AVN dysfunction occurred. During 12 months of follow-up, the patient has remained clinically free of symptoms.

As the differential diagnosis, concealed nodofascicular or nodoventricular bypass tracts, junctional ectopic tachycardia (JET), and intra-Hisian reentry should be generally considered in cases of supraventricular tachycardias with VA block.[2] In this case, the fact that the tachycardia was not reset by the ventricular extrastimuli during refractory of the His did not favor the existence of concealed bypass tracts. The reproducible induction by atrial extrastimuli, and the reproducible termination by ventricular extrastimuli and burst pacing supported AVNRT strongly rather than JET. Intra-Hisian reentry was not likely because the tachycardia was eliminated by RF applications in the SP area. Therefore, the diagnosis as AVNRT is considered appropriate.

We hypothesized that the RF applications at the SP area might have affected the properties of the UCP. Some investigators have reported that a definite UCP is not present;[3] however, we could not explain all these phenomena without the supposition of a certain common pathway between the atrium and AVNRT circuit in the present case. Furthermore, this hypothesis does not contradict the